



**HAL**  
open science

# The spatial distribution of the saturated hydraulic conductivity in the upstream part of the Merguellil watershed for the improvement of the hydrological modeling

Asma Hmaied

## ► To cite this version:

Asma Hmaied. The spatial distribution of the saturated hydraulic conductivity in the upstream part of the Merguellil watershed for the improvement of the hydrological modeling. *Hydrology*. 2022. hal-04584008

**HAL Id: hal-04584008**

**<https://hal.inrae.fr/hal-04584008>**

Submitted on 22 May 2024

**HAL** is a multi-disciplinary open access archive for the deposit and dissemination of scientific research documents, whether they are published or not. The documents may come from teaching and research institutions in France or abroad, or from public or private research centers.

L'archive ouverte pluridisciplinaire **HAL**, est destinée au dépôt et à la diffusion de documents scientifiques de niveau recherche, publiés ou non, émanant des établissements d'enseignement et de recherche français ou étrangers, des laboratoires publics ou privés.

Copyright

THE MINISTER OF AGRICULTURE,  
HYDRAULIC RESOURCES  
AND FISHING



MINISTRY OF HIGHER EDUCATION  
AND  
SCIENTIFIC RESEARCH



## NATIONAL AGRONOMIC INSTITUTE OF TUNISIA

Department of Rural Engineering, Water and Forests

MASTER'S THESIS

Speciality: Irrigation and Drainage

**The spatial distribution of the saturated hydraulic conductivity in the upstream part of the Merguellil watershed for the improvement of the hydrological modeling.**

Publicly defended by

**ASMA HMAIED**

**29 July 2022 In INAT**

In front of the jury composed of:

<b>Mr. Hedi Daghari</b> , Professor, INAT	President
<b>Mme. Ines Oueslati</b> , Assistant teacher, INAT	Supervisor
<b>Mr. Jalel Aouissi</b> , Assistant teacher, INAT	Assessor

## Abstract

Today, the climate crisis in the world is clearly related to water. It causes an increase in the variability of the hydrological cycle which eventually causes extreme weather events reducing the predictability of water resources and threatening the sustainable development of natural resources.

Hydrological abstraction such as infiltration is a fundamental parameter in the process of simulation and modeling of the water balance in a basin. These parameters allow us to analyze and determine the degree of reduction experienced by precipitation from the atmosphere to eventually become a runoff. However, the degree of knowledge of this abstraction is the product of our research process that will reduce the uncertainty that accompanies the results of all hydrological modeling.

In our work we aim to study the infiltration rate and map the saturated hydraulic conductivity in the upstream part of Merguellil watershed using two methods which are Beerkan and Mini-disc infiltrometer. The mini-disc infiltrometer has been more effective in some places with greater difficulty of access, and where the sand percentage is highly represented (sandy soils). On the other hand, Beerkan method also has been effective. In other parts the only limit was the amount of water required to perform the test and the availability of water.

The reliability of the results was assessed by the correlation coefficient (CC) that was equal to 0.96, the root mean square error (RMSE) that was equal to 23.0067 mm/h, and the Bias that was equal to 19.0014. By that, we can consider that the two methods were performing good enough to be used in further studies.

**Keywords:** Infiltration, saturated hydraulic conductivity, mini-disc infiltrometer, beerkan, spatial distribution, upstream part of Merguellil watershed

## Résumé

Aujourd'hui, la crise climatique dans le monde est clairement liée à l'eau. Elle provoque une augmentation de la variabilité du cycle hydrologique qui provoque à terme des événements météorologiques extrêmes réduisant la prévisibilité des ressources en eau et menaçant le développement durable des ressources naturelles.

Les prélèvements hydrologiques tels que l'infiltration sont des paramètres fondamentaux dans le processus de simulation et de modélisation du bilan hydrique d'un bassin. Ces paramètres nous permettent d'analyser et de déterminer le degré de réduction subi par les précipitations de l'atmosphère pour éventuellement devenir un ruissellement. Cependant, le degré de connaissance de cette abstraction est le produit de notre processus de recherche qui réduira l'incertitude qui accompagne les résultats de toute modélisation hydrologique.

Dans notre travail nous visons à étudier le taux d'infiltration et à cartographier la conductivité hydraulique saturée dans la partie amont du bassin versant de Merguellil en utilisant deux méthodes qui sont Beerkan et le mini-disque infiltromètre. Le dernier s'est montré plus efficace dans certains endroits plus difficiles d'accès, et où le pourcentage de sable est fortement représenté (sols sableux). Même aussi, la méthode Beerkan a également été efficace. Dans d'autres parties, la seule limite était la quantité d'eau nécessaire pour effectuer le test et la disponibilité de l'eau.

La fiabilité des résultats a été évaluée par le coefficient de corrélation (CC) égal à 0,96, l'erreur quadratique moyenne (RMSE) égale à 23,0067 mm/h et le biais égal à 19,0014. Enfin, les deux méthodes étaient suffisamment performantes pour être utilisées dans d'autres études.

**Mots-clés** : Infiltration, conductivité hydraulique à saturation, le minidisque infiltromètre, beerkan, répartition spatiale, la partie amont du bassin versant du Merguellil

## الملخص

اليوم ، من الواضح أن أزمة المناخ في العالم مرتبطة بالمياه. إنه يتسبب في زيادة تنوع الدورة الهيدرولوجية مما يؤدي في النهاية إلى أحداث مناخية شديدة تقلل من إمكانية التنبؤ بالموارد المائية وتهدد التنمية المستدامة للموارد الطبيعية.

يعتبر التجريد الهيدرولوجي مثل الارتشاح معلمة أساسية في عملية محاكاة ونمذجة توازن الماء في الحوض. تسمح لنا هذه المعلومات بتحليل وتحديد درجة الانخفاض الذي يعاني منه هطول الأمطار من الغلاف الجوي ليصبح في النهاية جرياناً. ومع ذلك ، فإن درجة المعرفة بهذا التجريد هي نتاج عملية البحث لدينا التي ستقلل من عدم اليقين المصاحب لنتائج جميع النمذجة الهيدرولوجية.

نهدف في عملنا إلى دراسة معدل التسلل ورسم خريطة التوصيل الهيدروليكي المشبع في الجزء العلوي من الحوض المائي "مرق الليل" باستخدام طريقتين هما « Beerkan » و "Mini-disk infiltrometer" .

. كان الMDI أكثر فاعلية في بعض الأماكن التي يصعب الوصول إليها ، وحيث تكون نسبة الرمال عالية (التربة الرملية) من ناحية أخرى ، كانت طريقة بيركان فعالة أيضاً. في أجزاء أخرى ، كان الحد الوحيد هو كمية المياه المطلوبة لإجراء الاختبار وتوافر المياه.

تم تقييم موثوقية النتائج من خلال معامل الارتباط (CC) الذي كان يساوي 0.96 ، وجذر متوسط الخطأ التربيعي (RMSE) الذي يساوي 23.0067 مم / ساعة ، والانحياز الذي كان يساوي 19.0014. أخيراً ، كانت الطريقتان تؤديان أداءً جيداً بما يكفي لاستخدامهما في دراسات أخرى.

**الكلمات المفتاحية:** التسرب ، التوصيل الهيدروليكي عند التشبع ، Beerkan ، mini-disque infiltrometer ، التوزيع المكاني ، الجزء العلوي من الحوض المائي "مرق الليل"

## *Acknowledgements*

The results presented in this thesis originate from the kind hospitality of many people that shared their time, knowledge, enthusiasm, abilities and friendship. I would like to sincerely thank all those who contributed scientifically and morally to support me during the development of this dissertation report. Everyone was so essential and unique, and every one was so kind and helpful. For all these reasons and more I kindly acknowledge you.

First of all, I would like to thank my supervisor *Mrs. Ines Oueslati*, and Mr. *Jalel Aouissi*, assistant teachers, for their patience, understanding, recommendations and valuable advice which helped me a lot in the completion of this work. Thanks also to their trust, I was able to fulfill my missions completely. They were of precious help in the most delicate moments.

A big thank you to *Mrs. Zeineb Kassouk* for her help during the data collection and all laboratory workers of soil direction in INGREF, especially *Mrs. Sana Dridif* for the good hospitality during my work there.

My sincere thanks also go to *Claude Hammacker*, *Pascal Podwojovski* and *Radhouane Hamdi* for their good friendship and support.

A big thank you to *Ines*, *Emna*, *Hela*, *Amal* for the good moments we shared together during my internship.

I present my respects to the president of the jury as well as to all the other members of the jury who were kind enough to examine this work.

I would like to thank my family and my friends *Ines*, *Emna*, *Hela* and *Amal* and all those who have contributed directly or indirectly to this project.

## *Dedication*

*My dear father Ahmed,  
who enlightened me on my way and who encouraged and,  
supported me throughout my journey,  
that he finds in this work the expression of my filial love and my eternal gratitude for the effort  
he made for my training  
I hope that this work will be for him the best reward.*

*My dear mother Naïma,  
the most affectionate and sweetest woman in the world  
who has been to me always a source of love and hope for her constant supervision, her great  
support and for all her sacrifices which will remain memorable.  
May God bless him with good health and long life.*

*To my sister Ines and my brothers Anis and Oussema  
  
who have loved, respected, supported and encouraged me throughout my life,  
who have always been by my side and,  
who have never ceased to be a source of happiness.*

*To my friends and colleagues  
For their listening, advice and encouragement and for all the pleasant moments that we  
shared together.*

*And to all who are precious.*

## **List of contents**

List of contents.....	
List of Images .....	
List of Figures .....	
List of Tables .....	
Introduction.....	
Chapter1: Bibliography.....	3
1. General characteristics of the soil.....	3
1.1. Introduction .....	3
1.2. Soil textures.....	3
1.3. Permeability of soil .....	4
2. Soil Hydrodynamic properties.....	4
2.1. Hydraulic conductivity.....	4
2.2. Factors that influence hydraulic conductivity .....	4
2.3. Orders of magnitude of hydraulic conductivity .....	5
3. Description of infiltration methods.....	5
3.1. Double ring infiltrometer method .....	6
3.2. Beerkan method.....	6
3.3. Mini-disk infiltrometer method .....	7
4. Sampling methods .....	9
Chapter 2: case study characteristics .....	11
1. Introduction .....	11
2. Description of the study area .....	11
2.1. Geological aspect .....	12
2.2. Climate .....	13
2.2.1. Temperature.....	13

2.2.2. Wind .....	14
2.2.3. Relative humidity .....	14
2.2.4. Evapotranspiration.....	15
2.2.5. Rainfall .....	15
2.3. Hydrological context .....	16
2.3.1. Hydrological functioning in Merguellil basin .....	18
2.4. The pedology .....	18
2.4.1. Soil texture.....	19
2.5. Water and Soil Conservation structures (CWS).....	21
Chapter 3: Materials and Methods .....	23
1. Introduction .....	23
1.1. In the laboratory .....	23
1.2. In situ.....	23
2. The adopted strategy and methodology, equipment and experimental protocol in our work	23
2.1. Description .....	23
2.2. Sampling.....	24
2.3. Bulk density determination .....	27
2.3.1. Equipment.....	27
2.3.2. Protocol.....	28
2.4. Initial water content determination .....	29
2.4.1. Equipment.....	29
2.4.2. Protocol.....	30
2.5. Granulometric test .....	31
2.6. Infiltration test protocol.....	32
2.6.1. Infiltration measures in the field.....	32
Chapter 4: Results .....	37

1. Spatial distribution of the sampling points .....	37
2. Sampling points physicochemical characteristics .....	38
3. The hydraulic conductivity curves by both methods beerkan and mini-disk infiltrometer 38	
3.1. Beerkan: .....	38
3.2. Mini-disk infiltrometer:.....	39
4. The bulk density results .....	40
5. The initial water content results.....	40
6. Granulometric results .....	41
7. The hydraulic conductivity map in the upstream watershed .....	45
8. Beerkan and mini-disc infiltrometer results comparison.....	47
Conclusions and perspectives .....	49
References .....	50

## **List of Images**

Image 1: Soil sampling using the auger .....	27
Image 2: (a), (b), (c) and (d) illustrating steps for bulk density determination.....	29
Image 3: (a), (b), (c) and (d) illustrating steps of initial water content determination.....	31
Image 4: Sedimentation step of the granulometric test.....	31
Image 5: (a), (b), (c) and (d) illustrating steps of beerkan infiltration method .....	33
Image 6: Mini-disc infiltrometer apparatus .....	34
Image 7: Field Measurements illustration.....	35

## **Abbreviations list**

**Ks**: the saturated hydraulic conductivity

**K**: the hydraulic conductivity

**MDI**: Mini-Disc Infiltrometer

**mm**: millimeter

**m.s<sup>-1</sup>**: meter per second

**DRI**: Double Ring Infiltrometer

**cm**: centimeter

**t**: time

**I**: Infiltration

**K<sub>0</sub>**: hydraulic conductivity for tension  $h_0$

**Φ<sub>0</sub>**: Wooding potential

**h**: suction heigh

**r**: disc radius

**s**: second

**Km<sup>2</sup>**: square kilometer

**Dj.**: Djebel

**m**: meter

**°**: degree

**°C**: degree celsius

**T**: Temperature

**Max**: maximum

**Min**: Minimum

**Hu**: Humidity

**%**: percentage

**ET<sub>0</sub>**: evapotranspiration

**NW**: North-West

**SE**: South-Est

**cm<sup>2</sup>**: square centimeter

**CWS**: Water and Soil Conservation structure

**M.ha**: million hectare

**SIG**: Geographical Information System

**REV**: Relative Elementary Volume

**h**: hour

**BD**: Bulk Density

**M**: mass of soil

**V**: volume

**Θ<sub>i</sub>**: Initial water content

**S**: sorptivity

**ms**: millisemence

**IDW**: Inverse Distance Weighted

**RMSE**: Root mini-square of error

**EC**: electrical conductivity

**CC**: correlation coefficient

## **List of Figures**

Figure 1: Different sampling approaches.....	9
Figure 2 : Merguellil watershed location.....	12
Figure 3: Interannual monthly temperatures of the Kairouan meteorological station from 2015 to 2019 (INM, 2019).....	14
Figure 4: The maximum, minimum and average humidity of the Kairouan meteorological station from 2015 to 2019 (INM, 2019).....	15
Figure 5: Annual and average precipitation of the Kairouan meteorological station from 1990 to 2013 .....	16
Figure 6 : Merguellil upstream hydrological network map.....	18
Figure 7 : Merguellil upstream pedology map.....	19
Figure 8 : Merguellil upsteam different textural classes map.....	20
Figure 9: Relation between texture diagram and hydraulic conductivity (Xanthoulis, FUSAGX).....	21
Figure 10 : Merguellil upstream Water and Soil Conservation structures map.....	22
Figure 11: Merguellil upstream pedology and texture classes maps .....	25
Figure 12: The 50-sampling points location template map .....	26
Figure 13: Sampling points spatial distribution map .....	37
Figure 14: Infiltration rate curves by beerkan method.....	39
Figure 15: Infiltration rate curves by mini-disc infiltrometer method.....	39
Figure 16: Merguellil upstream clay percentage distribution map .....	42
Figure 17: Merguellil upstream silt percentage distribution map.....	42
Figure 18: Merguellil upstream sand percentage distribution map .....	43

Figure 19: Textural distribution validation map .....	43
Figure 20: Hydraulic conductivity sampling points distribution map .....	45
Figure 21: Merguellil upstream hydraulic conductivity map by Beerkan method .....	46
Figure 22: Merguellil upstream hydraulic conductivity map by mini-disc infiltrometer .....	46
Figure 23: Beerkan vs mini-disc infiltrometer hydraulic conductivity comparison results.....	47
Figure 24: Scatter plot of hydraulic conductivity results using the two methods (mini-disc infiltrometer and Beerkan).....	48

## **List of Tables**

Table 1: Soil Types according to particles size (International Society of Soil Science) .....	3
Table 2: Soil classification according to the relative permeability (Calvet,2003).....	5
Table 4: Physicochemical characteristics results .....	38
Table 5: Bulk density results.....	40
Table 6: Water initial content results .....	41
Table 7: Granulometric results.....	44

## **Introduction**

The kinetics of water transfer processes in the unsaturated zone of the soil are of interest to many fields of study including agronomy. The management of water resources of a watershed, requires qualitative and quantitative data in the estimation of the hydrological balance. To describe and predict the transport of water in the unsaturated zone, knowledge of hydrodynamic properties is essential (**Wang *et al.*, 2013; Hu *et al.*, 2015; Beskow *et al.*, 2016; She *et al.*, 2017**).

The saturated hydraulic conductivity (Ks) presents the most important parameter, which has a direct influence on infiltration rate, of great importance for hydrological modeling. It determines the repartitioning of water at the surface into overland flow and infiltration (**Maier *et al.*, 2020**), thus impacting the runoff regime and soil erosion during high-intensity rainfall events (**Archer *et al.*, 2013; Zimmermann *et al.*, 2013**). The Ks also commonly acts as a conversion factor in unsaturated flow involving pore size distribution models (**Zhang and Schaap, 2019**), which is an essential tool in research of hydrological processes and in addressing water resource issues.

Generally, Ks is characterized by great spatial heterogeneity due to both the internal soil properties and external environmental conditions (**Huang and Shao, 2019**), which operate with different intensities at different scales (**Santra *et al.*, 2008; Sobieraj *et al.*, 2002**).

The mapping of Ks is essential to understanding soil water dynamics and is a sensitive input in hydrological modeling. the variability of soils, both spatially and temporally, because they contract, swell and undergo changes. This has long been recognized in soil science (**Jenny, 1941; Lin, 2006; Simonson, 1959; Wang and Shi, 2018**).

Many techniques that capture soil spatial and temporal variability have recently evolved to focus the attention of soil scientists on soil attributes related to hydrological models (**Qiao *et al.*, 2018; She *et al.*, 2017**). According to Libohova *et al.* (2018), the success of predictions when modeling hydrological processes depends on the accurate representation of the spatial and temporal variability of soil hydrological attributes and the main external factors, such as soil water dynamics. Ks is a key soil attribute for understanding the soil water movement phenomenon and is therefore one of the main inputs used in hydrological models. Several studies have reported that the spatial variability of Ks values in watershed is recognized as a complex phenomenon due mainly to the natural and anthropogenic processes that influence

soil water dynamic, predominantly at the surface layer (**Becker *et al.*, 2018; Baiamonte *et al.*, 2017; Wang *et al.*, 2013; Price *et al.*, 2010; Salemi *et al.*, 2013, Pinto *et al.*, 2019; Picciafuoco *et al.*, 2019).**

The hydraulic conductivity (K) is not a constant parameter and varies in time and space. It is reported to have the greatest statistical variability among different soil hydrological properties and can be induced by many factors (**Deb *et al.*, 2012; Wang *et al.*, 2013; Papanicolaou *et al.*, 2015; She *et al.*, 2017; Kanso *et al.*, 2018).** Moreover, it can strongly vary in time as was reported by Gupta *et al.* (2006). Heterogeneity of soil can be induced even by small-scale soil physical features such as fractures and wormholes, as was reported by Bockhorn *et al.* (2017) for low permeable clayey soils. Therefore, due to its highly variability as well as the effort required for Ks data sampling, representativeness of the spatial variability of Ks at the watershed scale is often difficult to obtain and can be costly (**Reichardt and Timm, 2020).**

There are numerous techniques available for determination of Ks and they can be divided into two major groups, based on whether they apply water to the soil at positive pressure (example: double ring infiltrometer, Beerkan) or negative pressure (example: mini disk infiltrometer, ...). In this study, the main aim was to assess and characterize spatial and temporal variability of the hydraulic conductivity of soil in Merguellil watershed. For this purpose, Beerkan method and mini disc infiltrometer (MDI) techniques were used.

# **Chapter1: Bibliography**

## **1. General characteristics of the soil**

### **1.1. Introduction**

A soil is composed primarily of minerals which are derived from parent material like rocks. Most of the mineral particles present in soils are composed of sand, silt, or clay. There are many characteristics that differentiate one soil from another. To work with soils, we need to understand the properties of soils. According to their size, soil particles are grouped into the following types, suggested by the International Society of Soil Science, mentioned in **Table1**:

*Table 1: Soil Types according to particles size (International Society of Soil Science)*

Types	Particle's size
Coarse particles or gravels	more than 2 mm diameters
Coarse sands	2 to 0.2 mm diameters
Fine sands	0.2 to 0.02 mm diameters
Silts	0.02 to 0.002 mm diameters
Clays	below 0.002 mm diameters

### **1.2. Soil textures**

The relative percentage of soil particle separations of a given soil is referred to as soil texture. Texture of soil for a given horizon is almost a permanent character, because it remains unchanged over a long period of time. The relative percentage of soil particles of average samples are almost infinite in possible combinations. It is, therefore, necessary to establish limits of variations among soil fractions so as to group them into textural classes which are defined by the granulometry method.

### **1.3. Permeability of soil**

The characteristic of soil that determines the movement of water through pore spaces is referred to as soil permeability. Infiltration is the vertical movement of water from the surface into the soil mass through the pores, while cumulative infiltration is the total amount of water that crosses the soil surface.

## **2. Soil Hydrodynamic properties**

### **2.1. Hydraulic conductivity**

By definition, hydraulic conductivity is the ability of the soil to transmit water through the porous medium (Hillel, 1998; Guellouz *et al.*, 2020). It depends on the type of soils, and impacts almost every soil application. It is critical to understanding the complete water balance. In a saturated environment, the displacement of water takes place in all interconnected pores. Otherwise, in an unsaturated environment, it takes place only in the continuous phase of water that does not occupy all pores. Conductivity in the middle unsaturated increases with water content to tend towards saturated conductivity.

Hydrologists need hydraulic conductivity values for modeling, and researchers use it to predict how water will flow through soil at different field sites. Agricultural decisions are based on hydraulic conductivity for determining irrigation rates or to predict erosion or nutrient leaching. The conductivity depends not only on the total porosity but also on the size of the conductive pores, it is higher for coarse sands than for clay soils where the pores are of smaller diameters (Calvet, 2003). For a saturated medium with stable structure, the hydraulic conductivity is of the order of  $10^{-5}$  to  $10^{-3}$  m.s<sup>-1</sup> in sandy soil and  $10^{-10}$  to  $10^{-8}$  cm.s<sup>-1</sup> in clayey soil (Hillel, 1998).

### **2.2. Factors that influence hydraulic conductivity**

The hydraulic conductivity is one of the most important hydraulic properties influencing water movement through soil. It is dependent on factors such as soil texture, particle size distribution, roughness, tortuosity, shape and degree of interconnection of water conducting pores. If we were only taking into account soil structure, coarser textured soils would typically have higher hydraulic conductivities than fine textured soils. However, soil structure and pore structure can have a significant impact on soil's ability to transmit water. A structured soil typically contains

large pores, while structureless soils have smaller pores (Qiao *et al.*, 2018; Yang and Wendroth, 2014).

### **2.3. Orders of magnitude of hydraulic conductivity**

It is useful to have benchmarks to locate the value of the hydraulic conductivity of the soil (Table 2), from a practical point of view. The limits cited by Calvet (2003) are generally used meanwhile it is not sufficient to fully describe the permeability of the soil:

*Table 2: Soil classification according to the relative permeability (Calvet,2003)*

Soil (according to the relative permeability)	Approximate range of saturated hydraulic conductivity (m.s <sup>-1</sup> )
Very low permeability	$K_s < 10^{-7} \text{ m.s}^{-1}$
Low permeability	$10^{-7} \text{ m.s}^{-1} < K_s < 10^{-6} \text{ m.s}^{-1}$
Average permeability	$10^{-6} \text{ m.s}^{-1} < K_s < 10^{-5} \text{ m.s}^{-1}$
High permeability	$10^{-5} \text{ m.s}^{-1} < K_s < 10^{-4} \text{ m.s}^{-1}$
Very high permeability	$10^{-4} \text{ m.s}^{-1} < K_s$

### **3. Description of infiltration methods**

Saturated hydraulic conductivity is one of the most important soil hydro-physical characteristics. Its determination is needed for many different applications and it is also one of the main input parameters for models simulating water transport through soil profile.

In situ infiltration measurement methods aim to know the flow vertical water in constant regime. The principle is based on the flow measurement seeping through a well-defined area of soil under a load constant hydraulic.

### **3.1. Double ring infiltrometer method**

The double ring infiltrometer (DRI) is a widely used method for infiltration test used in many applications (**Parr and Bertrand, 1960**). The infiltrometer consist of two concentric metal rings, which are driven into the soil, and of a perforated metal plate. The main source of error are the way of supplying water and the implantation of the ring, respect of the level of the water layer in the ring and stopping measurements before the soil has reached its maximum swelling.

#### **❖ Measurement procedure**

The measurement is taken in the inner cylinder, the outer cylinder is used only as a tool to ensure that water from the inner cylinder will flow downwards and not laterally. The soil surface in the inner cylinder is covered by a perforated metal plate which is used in order to dissipate the force of the applied water, to distribute water uniformly inside the ring and to prevent disturbance of the soil surface.

Two nail points of different lengths are fixed to the metal plate. These nails points are used for observation of decreasing water level during the infiltration. Both (inner and outer) cylinders are driven into the soil (to a depth of 10-20 cm). It is recommended that the turf around the ring's periphery is cut with knife, the soil then is less disturbed by driving the ring into it. The metal plate is placed on the soil surface in the inner cylinder, and water is poured into both cylinders (the water level in the inner cylinder should reach the upper nail point). At this moment, the stopwatch is started and the time needed for the water level to drop from the upper to the lower nail points is measured and recorded. After this elapsed time, a certain amount of water was infiltrated. When the water level reaches the lower nail point, the time is recorded and the same amount of water is poured back from a prepared graduated bottle. The water level in the outer cylinder is kept at the same level as the water level in the inner cylinder. Results from the DRI measurements can be taken only as directory information, however, they can be considered as accurate enough for many applications (**Matula et al., 1989**).

### **3.2. Beerkan method**

Beerkan method is based on field infiltration measurements (**Simunek et al., 1998; Angulo-Jaramillo et al., 2000; Jacques et al., 2002**). It permits to calculate the infiltration flow rate through the soil. The beerkan test is based on an axisymmetric three-dimensional infiltration with zero pressure loading and saturated water content at the soil surface.

#### ❖ **Measurement procedure:**

The beerkan infiltration method uses a simple annular ring. The surface of the soil on which the measure is applied must be plate. In natural soil case, the surface vegetation is removed while the roots remain in situ. Then the cylinder is positioned at the soil surface and inserted to a depth of about 1 cm to avoid lateral loss of the pounded water at the soil surface. A fixed volume of water is poured into the cylinder at time zero, and the time elapsed during the infiltration of the known volume of water is measured. When the first volume has completely infiltrated, a second known volume of water is added to the cylinder, and the time needed for it to infiltrate is recorded. This procedure is repeated consecutively until we reach the permanent regime. The measurements correspond to the accumulation of layers of infiltrated water as a function of time. Its layers of water are deducted by dividing the volume infiltrated by the surface of the ring. The experimental measurements make it possible to retrace the transitory and the permanent regime of the infiltration (**Lassabatere *et al.*, 2006**).

The advantage of the single ring infiltrometer method lies in the simplicity of the combination of the analysis methods.

### **3.3. Mini-disk infiltrometer method**

The mini-disk infiltrometer is a very handy, manually operated device to measure unsaturated hydraulic conductivity at tensions between -0.5 cm and -7 cm. It consists of two chambers, which are filled with water. The upper chamber controls the suction meanwhile water for infiltration is stored in the lower chamber.

#### ❖ **Measurement procedure**

A special care needs to be taken to the preparation of the soil surface. Good hydraulic contact must be established between the infiltrometer and the infiltration surface to get a correct measurement. When filling the infiltrometer with water, we do start with the upper chamber and then the water reservoir tube. We make sure that there is no leak of water from anyplace around the disk and then we set the suction rate. To start the experiment, we record the initial water level in the reservoir water tube, place the infiltrometer on the surface of the soil, and start the stopwatch. The water level must be recorded at regular time intervals or we can record the time laps for a regular water layer infiltrated.

### ❖ Calculation of Ks

The infiltration of water into the soil is described by the equation of Philip (1957). During the early stages of infiltration when soil suction is high, capillary flow dominates, and it is governed by square root function of time. In the latest stages of infiltration, when  $t$  is high, the water flow is mainly governed by gravity and follows linear kinetics.

For this steady regime phase, Wooding (1968) established an equation to describe the infiltration of water from a circular source:

$$I = k_0 + 4\phi_0 \times \pi \times r$$

Where,

$$\phi_0 = \int k(h) \cdot dh$$

$K_0$ : hydraulic conductivity for tension  $h_0$  (mm/s)

$\Phi_0$ : Wooding potential

$r$ : disc radius (cm)

$h$ : suction height (mm)

### ❖ Solving the equation

The equation has two unknowns  $K_0$  and  $\Phi_0$ , it can be solved if at least two different measurements are made with two different tensions  $h_1$  and  $h_0$ . The rate of infiltration is lower when the pre-set tension is lower. We establish the  $\frac{I}{\sqrt{t}}$  curves as a function of  $\sqrt{t}$  for the two tensions, where  $I$  is the infiltration (mm) and  $t$  is the time (s). Then the slope  $Q_1$  and  $Q_0$  of the curves  $\frac{I}{\sqrt{t}} = \sqrt{t}$  corresponding respectively to the tension  $h_1$  and  $h_0$  are determined. Then we calculate  $\alpha$  and  $K(h)$ .

$$\alpha = \frac{\ln\left(\frac{Q_0}{Q_1}\right)}{(h_1 - h_0)}$$

$$k(h) = \frac{Q_1}{(1 + (4 \times \pi \times r \times \alpha))}$$

Finally,  $K_s$  is determined from two parameters  $\alpha$  and  $K(h)$  already calculated.

$$k_s = \frac{k(h)}{\exp(\alpha \times h)}$$

#### 4. Sampling methods

Sampling entails selecting a subset of individuals from the total population to be measured, the measurements obtained on this subset (or sample) will then be used to estimate the parameters of the total population. Sampling is fundamental in any soil science field research program because measuring the entire population is difficult in any realistic study.

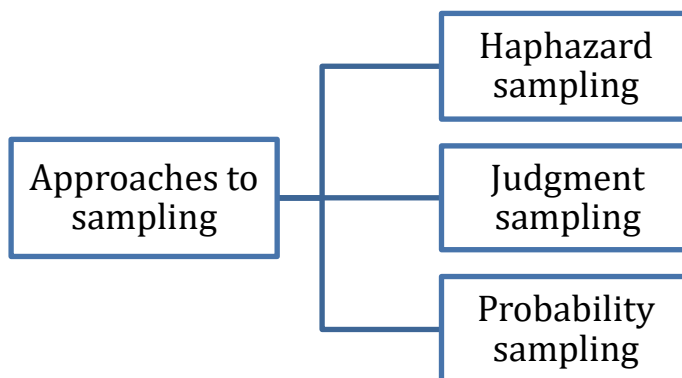


*Figure 1: Different sampling approaches*

Haphazard sampling, judgment sampling, and probability sampling can be all used to select sample locations. Haphazard, accessibility, or convenience sampling entails the sampler, making a series of nonreproducible, idiosyncratic judgments with no systematic attempt to

verify that the samples taken are representative of the population being sampled. This type of sampling is diametrically opposed to scientific sample designs. Judgment sampling (also known as purposive sampling (**De Gruijter, 2002**), entails selecting sampling places based on knowledge held by the researcher. Although judgment sampling can yield reliable estimates of population parameters such as averages and totals, it cannot offer a measure of the precision of these estimates (**Gilbert, 1987**). Furthermore, the estimate's reliability is not only as good as the researcher's assessment. Using a variety of unique sample layouts, probability sampling selects sampling points at random places, and the chance of sample point selection may be computed for each design. Unlike judgment sampling, this permits an estimate of the correctness of the parameter estimates to be made. This allows a range of statistical analyses based on the estimates of variability of the mean to be used, and it is by far the most common type of sampling in soil science.

## **Chapter 2: case study characteristics**

### **1. Introduction**

This chapter is broken into two sections. The first is devoted to a description of our study location (Kairouan region and precisely Merguellil watershed), namely a description of the geographical environment and a description of the climatic setting. In the second section, we present the various forms of experimental and spatial data that were collected and used in the context of this research.

### **2. Description of the study area**

Merguellil watershed is located between latitudes 35°25'40" North and 35°51'10" North, and longitudes 9°09'00 East and 9°46'30" East. The upstream basin, covering an area of 1200 Km<sup>2</sup>, is based on the southern slopes of the Tunisian ridge. It is characterized by strong geological heterogeneity with the dominance of plains and plateaus in its middle zone and it is surrounded by mountains called Djebels (Dj.). The hypsometry varies between 1226 m and 200 m altitude from west to east. It is limited to the north by the southern fallout of Dj. Ousslet and the Dj. Djebil, to the south by the El Ala plateau and the Dj. Barbou, to the west by the highlands of Kesra and to the east by the Dj. Ousslet, Dj. Chrechira, Dj. El Houareb and Dj. Touilla.

At the El Houareb dam, built in 1989 to protect the city of Kairouan from flooding and to supply future irrigated areas in the plain, there is water and soil conservation structures as well as 38 hill lakes and 4 hill dams.

We recall that the upstream zone of the Merguellil watershed includes part of six delegations: the delegations of Haffouz, El Ala, Oueslatia and Hajeb El Layoun are located in the governorate of Kairouan, the delegations of Makthar and Kesra are in the governorate of Siliana.

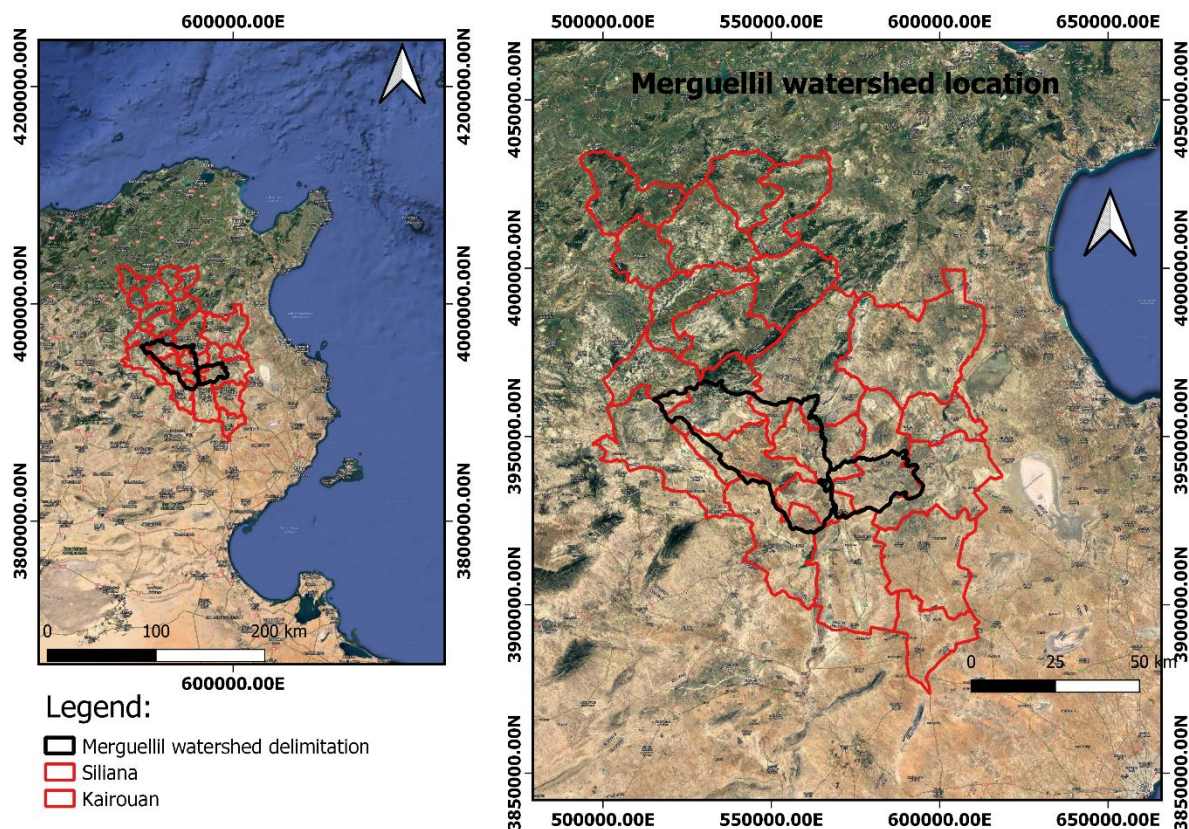


*Figure 2 : Merguellil watershed location*

## 2.1. Geological aspect

The ridge stretches over 190 km<sup>2</sup> upstream of the basin (Dj. Kesra and Dj. Barbrou) to the escarpments of El Garia and Dj. Shkira in the northern section of the watershed. The elevations range from 700 to 1226 m. This areas terrain is extremely rough. Many streams have cut their beds through limestone rocks and relatively soft marly, resulting in escarpments topped by some summits in spots (**Hamza, 1983**). The middle section of the watershed is nearly flat sequence of plains and plateaus that are slightly dissected and are bordered to the south by Wadi Mora. Finally, in the basins most downstream region, the high steppes occupy 680 km<sup>2</sup> at altitudes ranging from 200 to 400 m. They correspond to the foothills of the Ouslat and Trozza Dj., as well as the northern piedmont of Dj. Touila. The watershed in this area is bounded to the east by the Dj. Cherichira and the Kairouan plain.

The slopes of the Merguellil basin are varied. Flat terrain (0° to 5°) prevails in the middle (80 percent of the basin area). Weak slopes (5° to 10°) may be found in the El Ala, Haffouz, and Dj.Ouslat foothills. Slopes of more than 10° are found in the western section of the basin. The Merguellil watersheds geology is complicated. It is characterized by silts, sands, clays, gravel,

and calcareous crusts which are concentrated in the upper basin, the Zebbes sub-basin, and around the El Houareb dam (**Ouali, 1985; Bouzaiane and Laffrogue, 1986, Chadly, 1992**).

## **2.2. Climate**

The location of Merguellil watershed is susceptible to a variety of climatic effects. Indeed, it is under the influence of two extremely different climatic zones: the north of Tunisia, which has a cold damp and subhumid climate, and the south, which has an arid and desertic environment. Thus, the north-western part of Merguellil has a semi-arid climate that is both inferior and superior to a cold winter, while the remainder of the basin has a semi-arid climate that is superior to temperate winter. The Merguellil watershed is located in a climatic transition zone between the north which is under the Mediterranean influence with predominant winds from the north and is generally mild and humid, and the pre-Saharan zone to the south, which is hot and dry (**Bouzaiane and Laffrogue, 1986**).

### **2.2.1. Temperature**

Usually the coldest months are December, January and February. The hottest months are July and August. According to data from the Kairouan meteorological station for the 5 years from 2015 to 2019, we see that the average temperature varies between 13°C and 32°C. The coldest month is February while the hottest months are July and August (Figure3). In addition, in the Merguellil watershed, temperatures decrease with altitude and increase from upstream to downstream with an average gradient of 0.4°C / 100 meters above sea level, that justifies the aridity of the climate (**Lacombe, 2007; Bouzaiane and Laffrogue, 1986**).

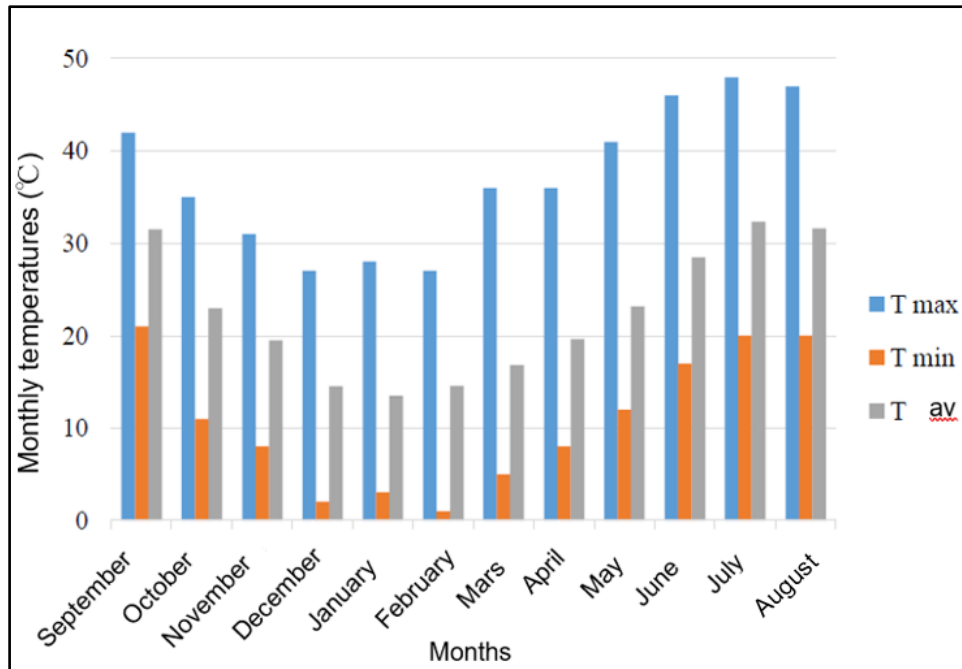


**Figure 3: Interannual monthly temperatures of the Kairouan meteorological station from 2015 to 2019 (INM, 2019)**

### **2.2.2. Wind**

According to the Kairouan weather station, the prevailing wind blows from the north and north-west sector in winter and from the south and south-west sector in summer. Winds are generally light. There are two characteristic winds of the region:

- The sirocco is a hot and dry wind of Saharan origin often accompanied by sand. It blows between the months of April and September and causes significant temperature increases of up to 50°C.
- The jebbali is a cold winter wind. It originates in the Algerian massifs (**Bouzaiane et al., 1986**).

### **2.2.3. Relative humidity**

The average monthly relative humidity in the region fluctuates between 55% and 70% during the cold season and between 40% and 55% during the warm season. The climate is therefore moderately dry from September to April and very dry from May to August. This explains the atmospheric clarity (**Bouzaiane and Lafforgue, 1986**). The figure 4 shows the curve that presents the monthly averages of the maximum and minimum daily relative humidities recorded in the Kairouan meteorological station from 2015 to 2019.

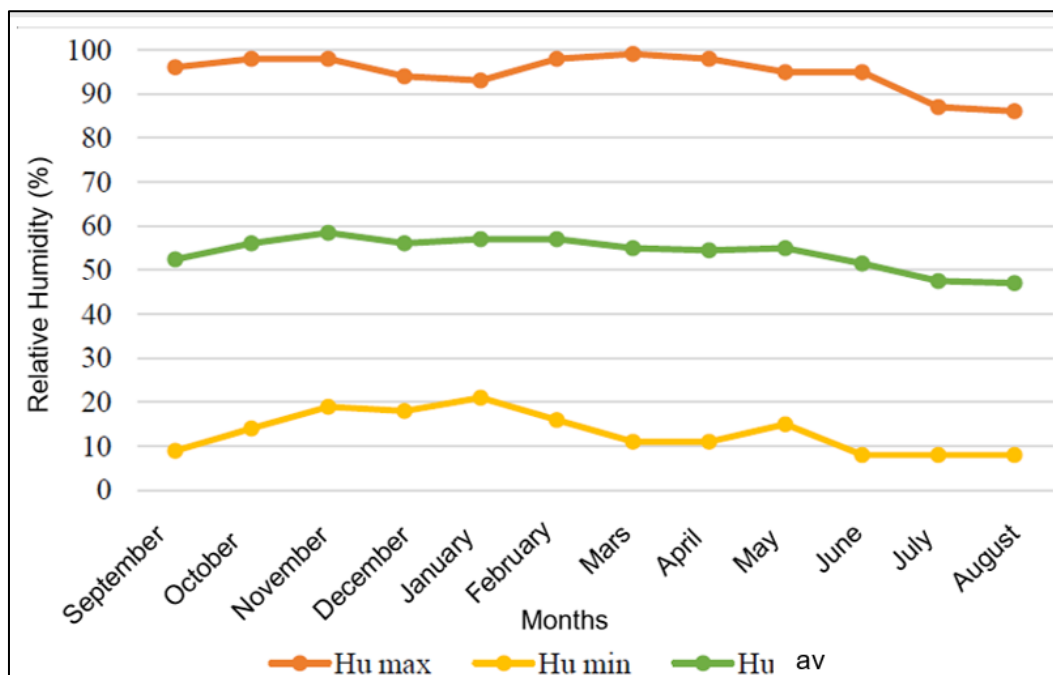


**Figure 4: The maximum, minimum and average humidity of the Kairouan meteorological station from 2015 to 2019 (INM, 2019)**

#### **2.2.4. Evapotranspiration**

It depends mainly on temperature, air humidity and wind. In the Merguellil basin, the evaporation measured (using 12 evaporation tanks installed at the edge of each hill reservoir of the HYDROMED network) varies between 1492 mm/year ( $ET_0 \sim 895$  mm/year) at the Janet station which is located at a distance of 2.2 km northwest of Makthar and at an altitude of 810 m and 2120 mm/year ( $ET_0 \sim 1272$  mm/year) at the El Houareb dam. Maximum evaporation in summer in the lowest areas, and minimum in winter in the higher areas. Nearly 50% of annual evaporation takes place during the three summer months (June, July and August) (Guillaume, 2007).

#### **2.2.5. Rainfall**

The Merguellil watershed is characterized by interannual and spatial variability of a very heavy precipitation. The average annual rainfall varies between around 500 mm/year in Makthar and less than 300 mm/year in Kairouan (Leduc *et al.*, 2007; Ogilvie *et al.*, 2014). The rains are

frequently torrential, especially in September and March, causing intense runoff and severe erosion which reduces the storage of water in the soil (**Ben Ammar, 2007**). The rainy season lasts for nine months from September to May, the months of June, July and August are dry, but with stormy rain sequences of very high intensity. Indeed, the area of the Kairouan plain is classified among the areas most dangerously threatened by the variability of rainfall, this is the case of the both exceptional and devastating floods that occurred in the fall of 1969 (**Kingumbi, 2006; Ben Boubaker et al., 2003; Alazard, 2013**).

According to the Kairouan meteorological station, it can be seen that the rainfall varies between 493 mm and 106 mm during the period 1990-2013, while the average rainfall in the area is around 284 mm (Figure5).

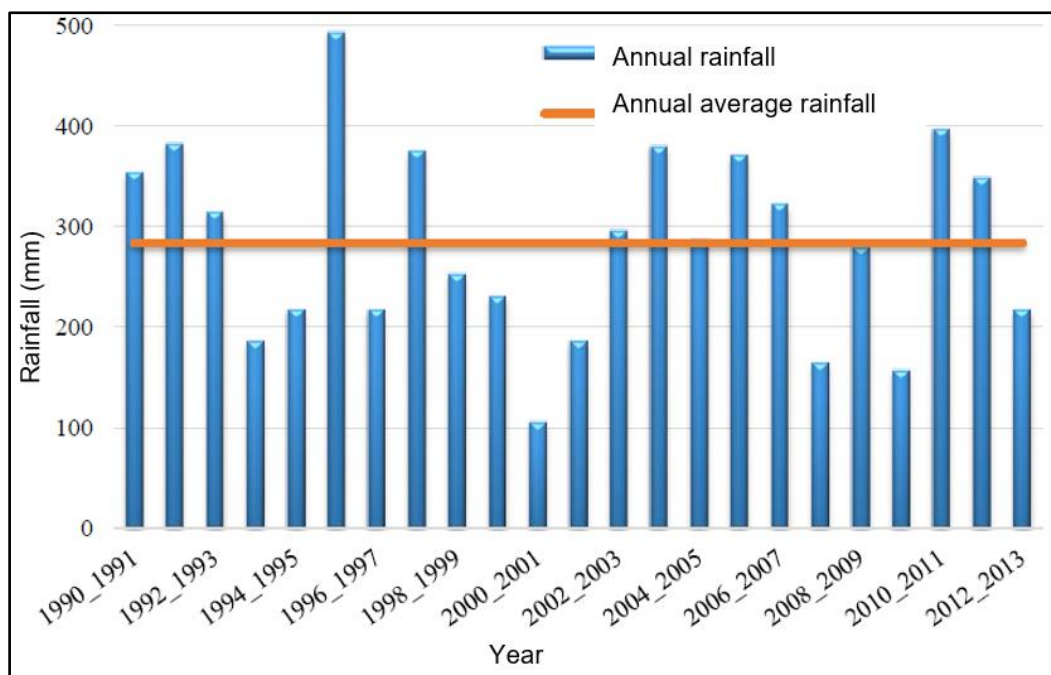


**Figure 5: Annual and average precipitation of the Kairouan meteorological station from 1990 to 2013**

### **2.3. Hydrological context**

According to Castany (1968), Besbes (1975; 1976), Chaieb (1988), and Mansour (1995; 1997), the aquifer of the plain of Kairouan is considered the most important reservoir of the central Tunisia (approximately 3000km<sup>2</sup>), housing several aquifers stacked on top of each other and communicating with each other more frequently (Figure6). The Merguellil basin is almost always endorheic and its natural outlet was Sebket El Kelbia located northwest of the city of

Kairouan (**Bouzaiane and Lafforgue, 1986**). The main stream of the Merguellil originates in the mountainous area of Makthar. The Oued generally flows in a North-West and South-East (NW-SE) direction in the watershed to reach the outlet which is the El Houareb dam. The El Houareb dam now prevents flows from reaching the plain and the dam can be considered as the new end of upstream surface flows.

Like most of the Oued in Tunisia, Oued Merguellil successively takes several names. First of all, it is Oued Bahloul which drains the high plateau of Kesra in the Makthar region. Then, Oued Kerd which takes over at Oueslatia and then it becomes Oued Merguellil. At Haffouz, Oued Merguellil receives the waters of its tributary Oued Zebbes which is the most important tributary of Merguellil and which drains the northern slope of Djebel Trozza as well as the plateau of El Ala.

Since 1960s, five hydrometric stations have been installed on the rivers of Merguellil basin. These are upstream to downstream of the station of Skhira, Zebbes, Haffouz, Sidi-Boujdaria and El Houareb. The Merguellil Oued receives water from several tributaries, of which the most important are (**Hamza, 1976; Ben Ammar, 2007; Alazard, 2013**):

\_ Oued Zebbes, which drains an area of 181 km<sup>2</sup> of El Ala plateau with relatively gentle relief.

\_ Oued El Hammam which owes its name to the thermal springs of Ain El Hammam, and whose watershed covers 27 km<sup>2</sup>.

\_ Oued Hoshas, whose watershed of 36 km<sup>2</sup> drains the eastern and south-eastern part of Dj. Trozza.

\_ Oued Ben Zitoun which drains 109 km<sup>2</sup>. It only reaches the Merguellil Oued during the strongest floods.

\_ Oued El Khechem, which drains the western flank of the Dj. Touilla and rarely reaches the Merguellil Oued.

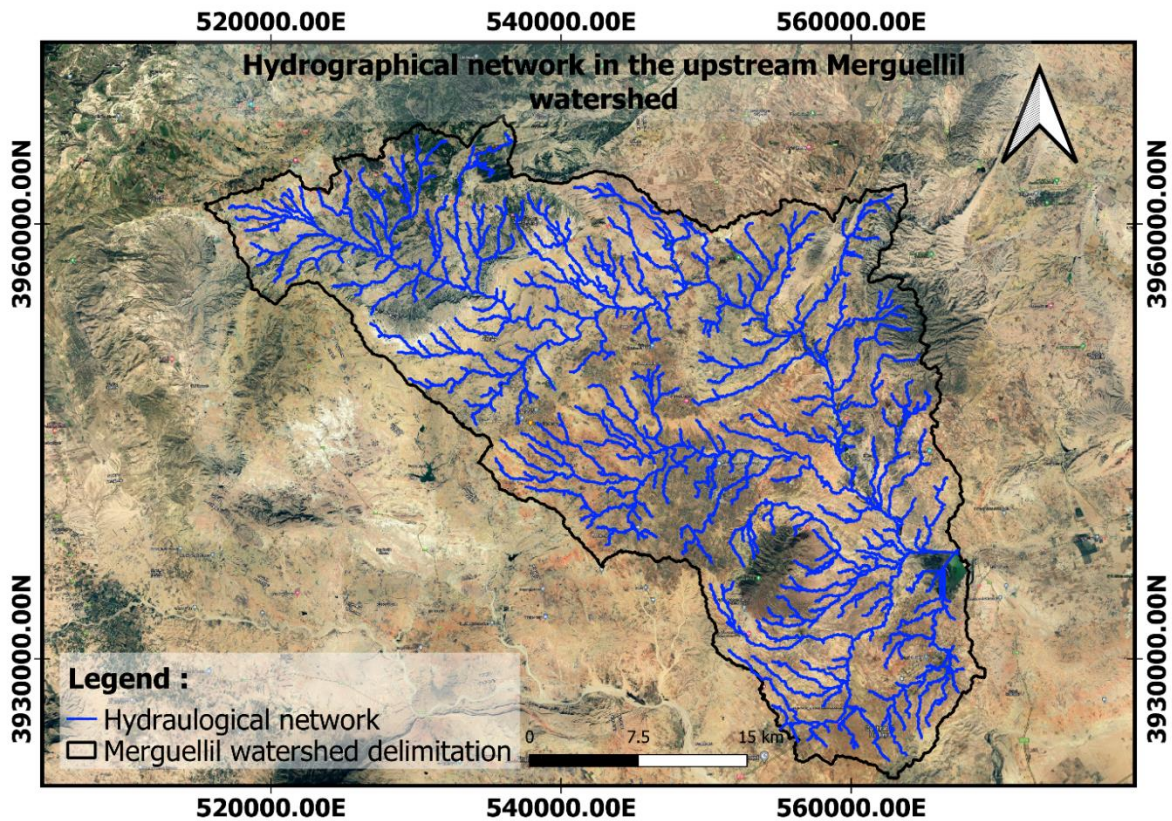


*Figure 6 : Merguellil upstream hydrological network map*

### **2.3.1. Hydrological functioning in Merguellil basin**

The floods of the Merguellil Oued are very rapid and violent, the stormy nature of the rain's upstream area produces an immediate runoff and rapid transfer to the Kairouan plain (**Hamza, 1988**). The flow of the Oued is characterized by extreme spatial and temporal variability. The course of Merguellil Oued can be divided into two sections: a first quasi-permanent section where the flow is supported by multiple sources and a second section from the region of Khit El Oued, where alluvium becomes more abundant promoting rapid water infiltration (**Bouzaiane and Lafforgue, 1986; Kingumbi, 2006**).

### **2.4. The pedology**

The soils of the Merguellil watershed are primarily composed of bedrock degradation. In relation to the low density of the plant cover, the humus and clay-humic complexes contents is low. They are poor and thin because they have been exposed to severe erosion (**Barbery and Mohdi, 1987, Mizouri et al., 1990**).

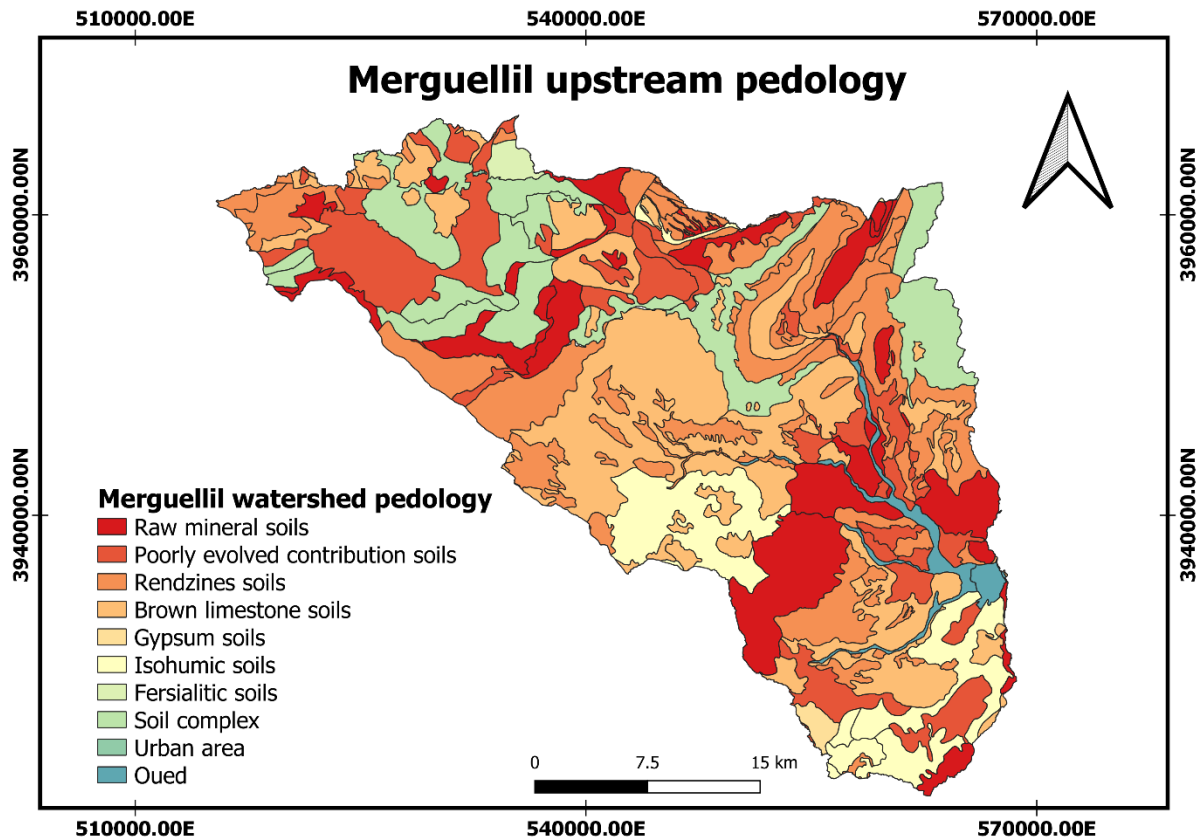


*Figure 7 : Merguellil upstream pedology map*

According to the pedology map (**Figure 7**), raw mineral soils, poorly evolved contribution soils, rendzines, brown limestone soils, gypsum soils, isohumic, fersialitic, and soil complex are the eight main pedology classes that exist in the upstream zone of Merguellil watershed.

### **2.4.1. Soil texture**

Our study area is almost characterized by three dominant textural classes (**Figure 8**): sandy soils present an average of 42,13%, sandy-loam soils present 50,53% and the clayey-loam soils present 7,34%. These different textural classes are distributed all over the upstream zone in heterogeneously way.

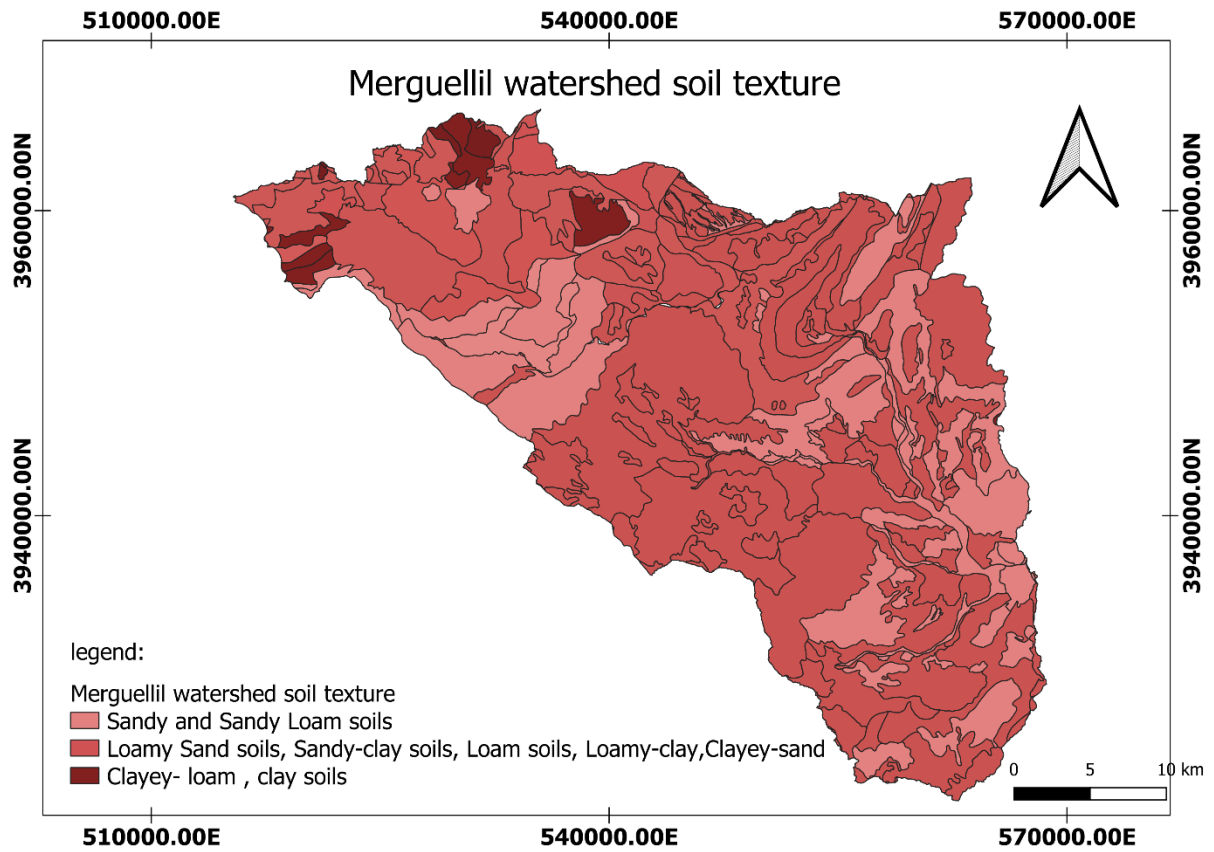


*Figure 8 : Merguellil upstream different textural classes map*

The soil texture is strongly related to the hydraulic characterization of the soil specially the hydraulic conductivity as it is shown in **Figure 9**:

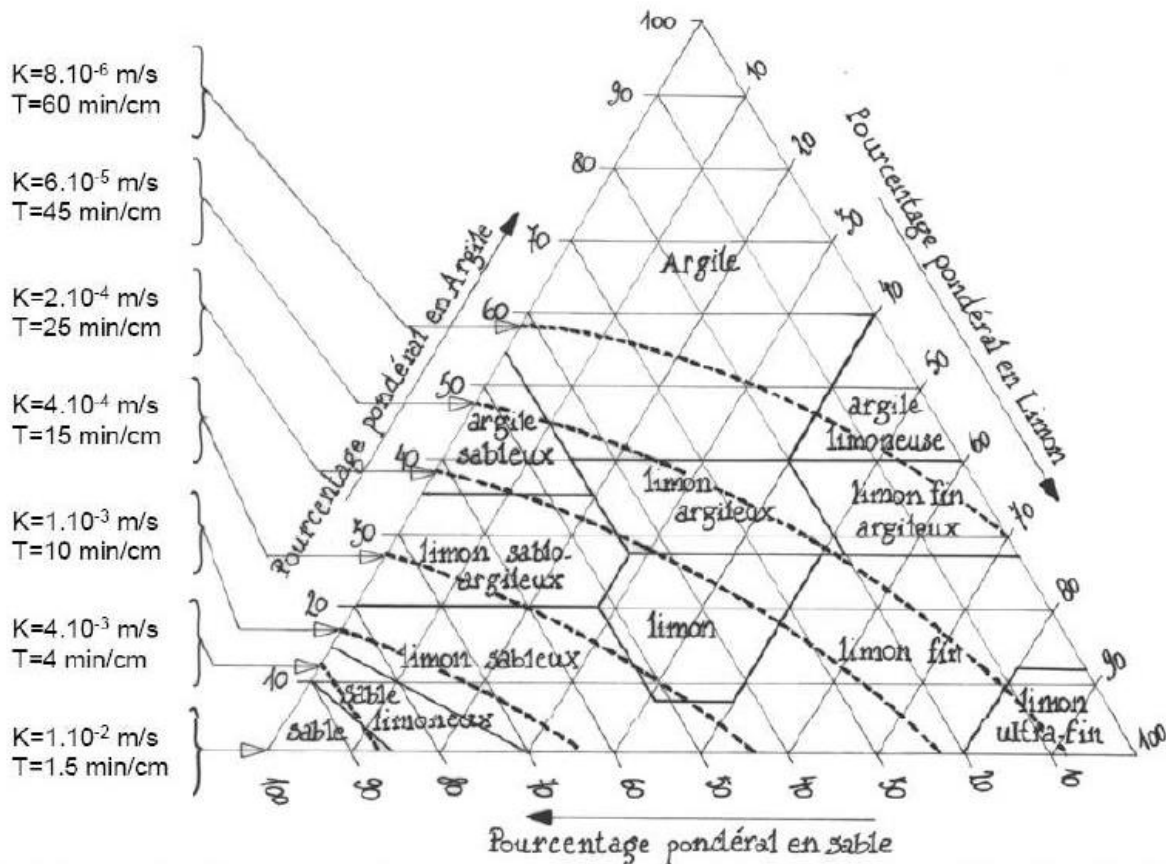


**Figure 9 : Relation between texture diagram and hydraulic conductivity (Xanthoulis, FUSAGX)**

## **2.5. Water and Soil Conservation structures (CWS)**

The CWS were carried out in the 1960s, as part of a major CWS development program along the Tunisian Ridge providing the construction of more than 850 hill reservoirs and the development of 1 M.ha by anti-erosion benches (Nasri, 2007). Further work by CWS was undertaken under the ten-year strategy (1991-2000) and two development programs funded by the European Union (FIDA, 2004). Pastoral plantation, earthen benches (embankments perpendicular to the slope) and dry rock sills are the slopes most often observed in the basin (Dridi, 2000). Most of the benches are located in the middle zone of the basin, with 70% in the Haffouz sub-basin (Kingumbi, 2006). The development of watercourses is mainly hill lakes and hill dams. The CWS expanded rapidly after 1989 (Lacombe *et al.*, 2008). The total developed area increased by 4% in 1970 (Ben Mansour, 2006) to 19% in 2011 (Mechy, 2013) of the entire basin areas (1200 km<sup>2</sup>) (Figure 10).

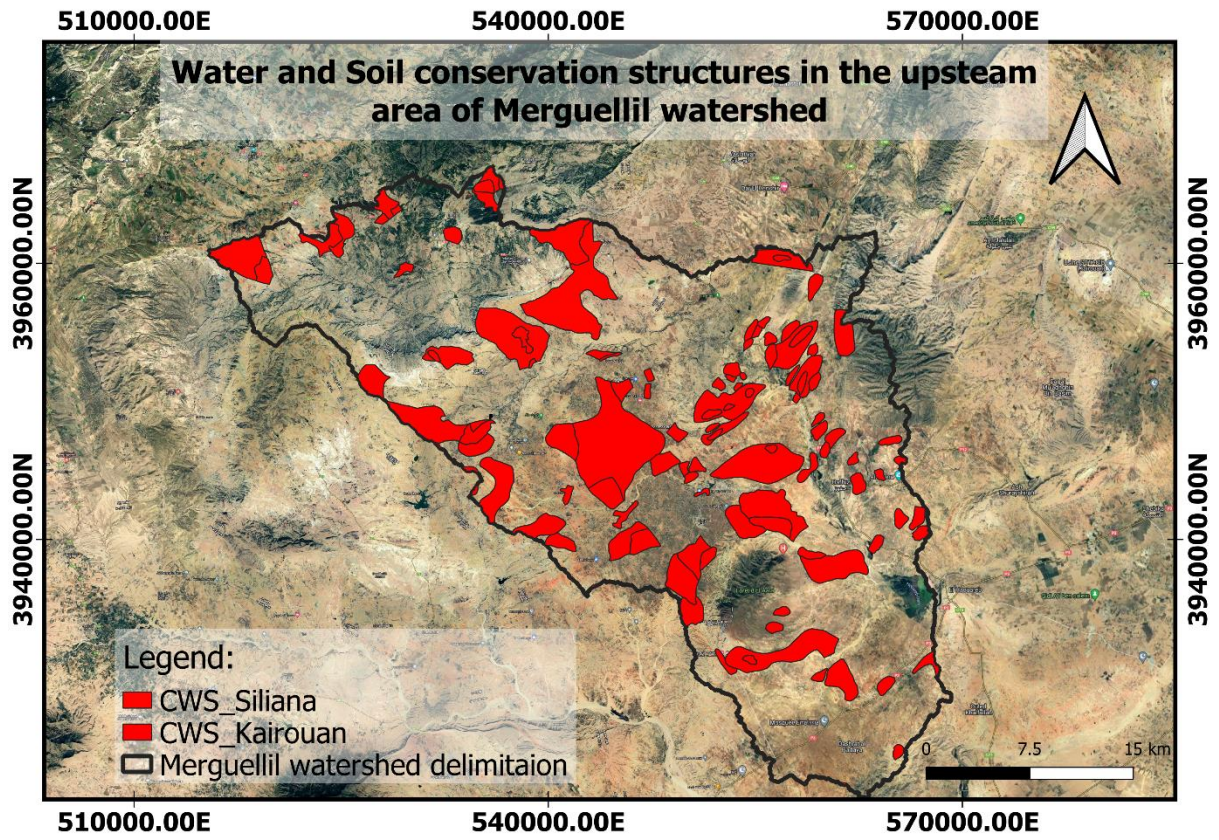


*Figure 10 : Merguellil upstream Water and Soil Conservation structures map*

## **Chapter 3: Materials and Methods**

### **1. Introduction**

The hydraulic conductivity (K) is a physic parameter that conditioning water infiltrability through the soil and, then, the infiltration rate. This parameter can be directly measured in situ which is the case in our study for which our main goals are:

#### **1.1. In the laboratory**

- Determination of the bulk density and the initial water content in the soil at each sampling location.
- Determination of the granulometric distribution at each sampling location.
- Determination of the physicochemical characteristics.

#### **1.2. In situ**

- Determination of K on the surface of different presented soils in our study area (the upstream of Merguellil watershed).
- Determination of the cumulative infiltration.
- ➔ The spatialization of K obtained after data treatments.
- ➔ Creation of the card of the spatial distribution of the saturated hydraulic conductivity characteristic of our study area.

## **2. The adopted strategy and methodology, equipment and experimental protocol in our work**

### **2.1. Description**

To achieve our goals we, as a first step, have done a preliminary analytic study to our study area.

- ❖ Study area analysis

It is essential for the establishment of scientific approach and then it permit to have a first field approach. This work allows the verification of the study area and its accessibility.

### ❖ Office work

Analysis of different documents such as articles, masters, thesis...

The collection of SIG data from the agricultural map of Kairouan, 2004 in order to create the following maps:

- Merguellil watershed delineation map.
- Soil texture map in the watershed.
- Map of the soil pedology in the watershed.
- Hydrographic network map in the watershed.
- Water and Soil conservation structures map in the watershed.

### ❖ Field work

Thanks to the GPS-Waypoints and MAPinr applications we were able to save time when positioning our sampling points.

The transfer of coordinates from both applications GPS-Waypoints and MAPinr to the geographical information system (SIG).

(.csv) ----- > (.shp)

(.kmz) ----- > (.shp)

The first visits serve to verify the field accessibility supported by surveys carried out with farmers in the study area. When it comes to owned farms, the agreement of the farmer is essential to settle in his plot.

## **2.2. Sampling**

The characterization of sites often requires sampling and analysis of soils in order to appreciate the spatial distribution. Sampling is the entire process aimed at producing representative samples of an initial environment. The objective of the sampling is to be as representative as possible of the environment it is supposed to represent. The quality of this step is crucial because it conditions a large number of decisions.

In our work, we will consider that every soil unit (sample) is homogeneous and which the size of the representative elementary volume (REV) is valid for its physics and hydrodynamics properties.

### ❖ Sampling strategy:

\* Preliminary study, based on the three created maps (**Figure 11**), (Merguellil watershed delimitation, pedology classes, texture classes).

\* Making a soil sampling plan, taking-in a consideration of a good spatial repartition of the sampling points location in a way that can cover almost the majority of our study area. The main characteristics of sampling plan are as follows:

- \_ The number of sampling points (the optimization according to the targeted objectives, the size of the site, the desired degree of precision).
- \_ The depth of samples.
- \_ The type of samples to be taken.
- \_ The arrangement of sampling points.

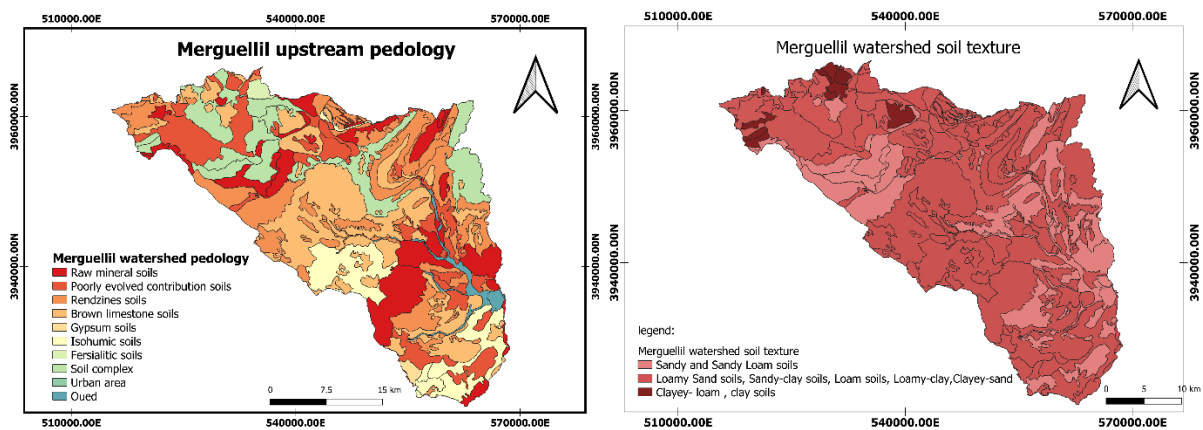


**Figure 11: Merguellil upstream pedology and texture classes maps**

Our first tentative to have a sampling repartition led to what is shown below in the map (Figure 12):

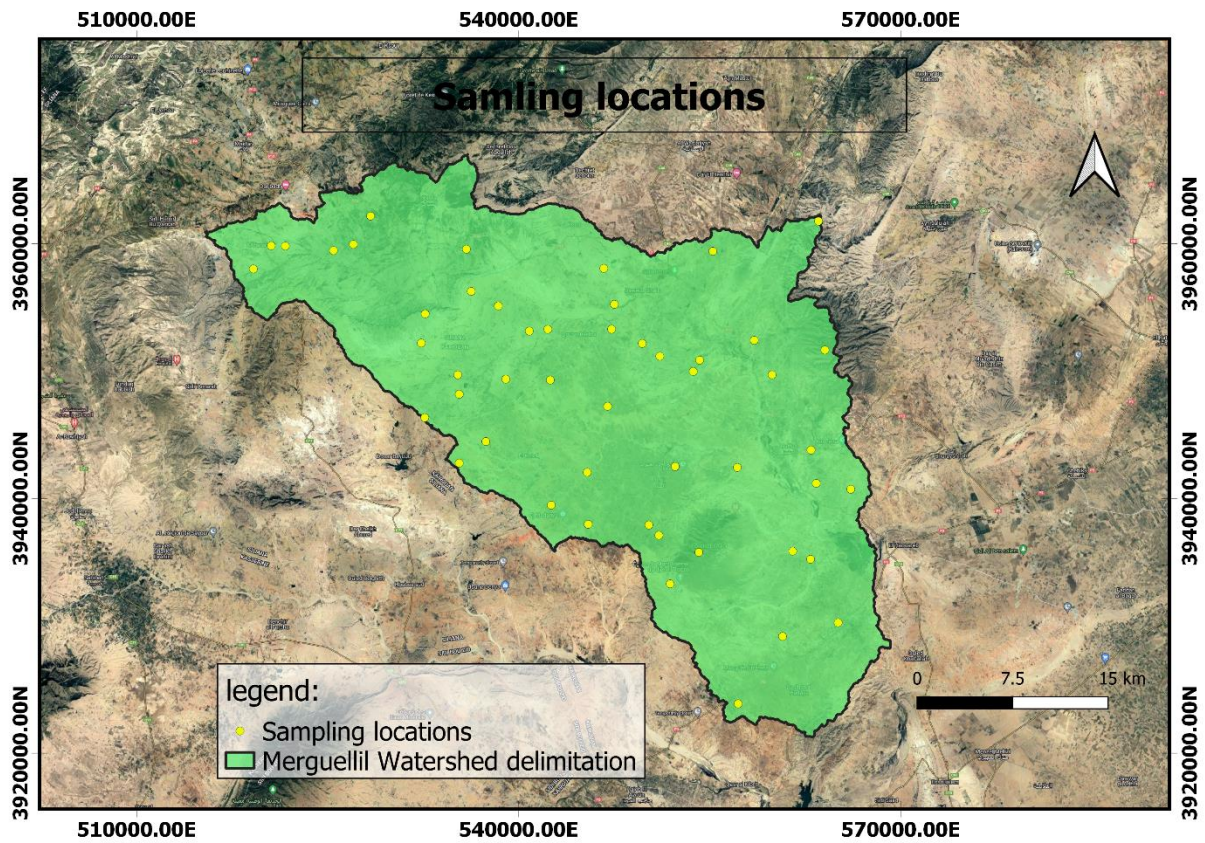


*Figure 12: The 50-sampling points location template map*

❖ Sampling technique:

The choice of sampling technique used is depending on the nature, the volume and the depth of the sample to be collected. In our work, we are only considered by the 20 cm depth of soil for this we are using an auger which is a low-cost sophisticated sampling device and fast for reduced depth (**Image1**).



*Image 1: Soil sampling using the auger*

❖ Sampling points:

For the experimental area a total of **50** analysis points were defined for the upstream area of Merguellil watershed. The location of the sampling points has been defined based on accessibility criteria, types of soils and water availability for the use of Beerkan (simple ring infiltrometer). Each point is accorded to an ID number, altitude and longitude coordinates.

### **2.3. Bulk density determination**

Bulk density (**Image 2**), is the weight per unit volume, generally expressed in grams per cubic centimeter ( $\text{g}/\text{cm}^3$ ). It corresponds to the dry weight of a volume of soil whose structure has not been disturbed. It is also the mass of a unit volume of soil dried at  $105\text{ }^\circ\text{C}$  for 48 hours in the oven. This volume includes solids than pores. It is measured by the cylinder method using the disturbed samples, knowing the constant dry weight of the samples at  $105\text{ }^\circ\text{C}$  and the volume of the sample cylinder used (**Blake and Hartage, 1986**).

#### **2.3.1. Equipment**

\*Cylinder

\*Metal trowel

\*Hammer

\*Hermetic plastic bags

\*Containers

### **2.3.2. Protocol**

- Insert the sample cylinder into the soil using a hammer.
- Carefully extract the cylinder. It may be necessary to insert a shovel behind the cylinder to ensure that no soil falls.
- Empty the cylinder content into a plastic bag.
- Dry the soil sample, emptied previously, in the oven at 105 °C for 48h.
- Obtain the dry weight of the soil sample.
- Calculate the bulk density via the formula mentioned below:

$$BD = \frac{M_{Dry\ soil}}{V_{cylinder}}$$

With BD: bulk density (g/cm<sup>3</sup>)

M<sub>dry soil</sub>: mass of soil dried in the oven (g)

V<sub>cylinder</sub>: cylinder sampler volume (cm<sup>3</sup>)



*Image 2: (a), (b), (c) and (d) illustrating steps for bulk density determination*

## **2.4. Initial water content determination**

This test is performed to determine the water content of soils. The water content is the ratio, expressed as a percentage of the mass of water in a given mass of soil to the mass of the dry soil (Mermoud, 2006).

### **2.4.1. Equipment**

- \*Drying oven
- \*Balance
- \*Containers

\*Spatula

### 2.4.2. Protocol

The initial water content (**Image3**), is estimated by measuring the difference between the fresh weight and the dry weight. Its procedure is very simple. Just take out a sample from soil, take its weight and put it into the oven for 24 hours then take it out and take its weight again. The difference of weight will be the weight of water present in the soil sample (**Pauwels *et al.*, 1992**) according to the following formula:

$$\theta_i(\%) = \frac{M_{Fresh\ soil} - M_{Dry\ soil}}{M_{Dry\ soil} - M_{Container}} \times 100 \times BD$$

With

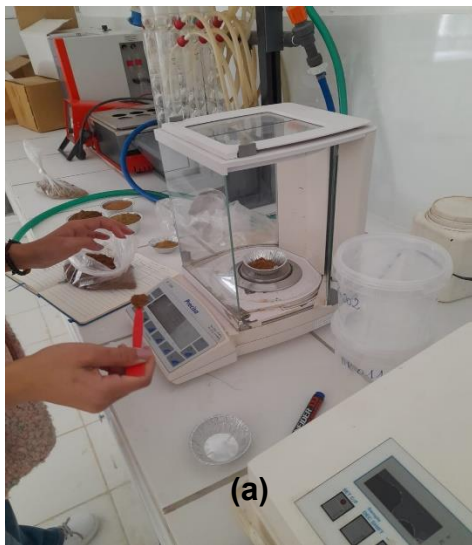
$\Theta_i$ : initial water content (%)

$M_{Fresh\ soil}$ : mass of the fresh soil (g)

$M_{dry\ soil}$ : mass of soil dried in the oven at 105 C for 24h (g)

$M_{container}$ : mass of the empty container (g)

BD: bulk density



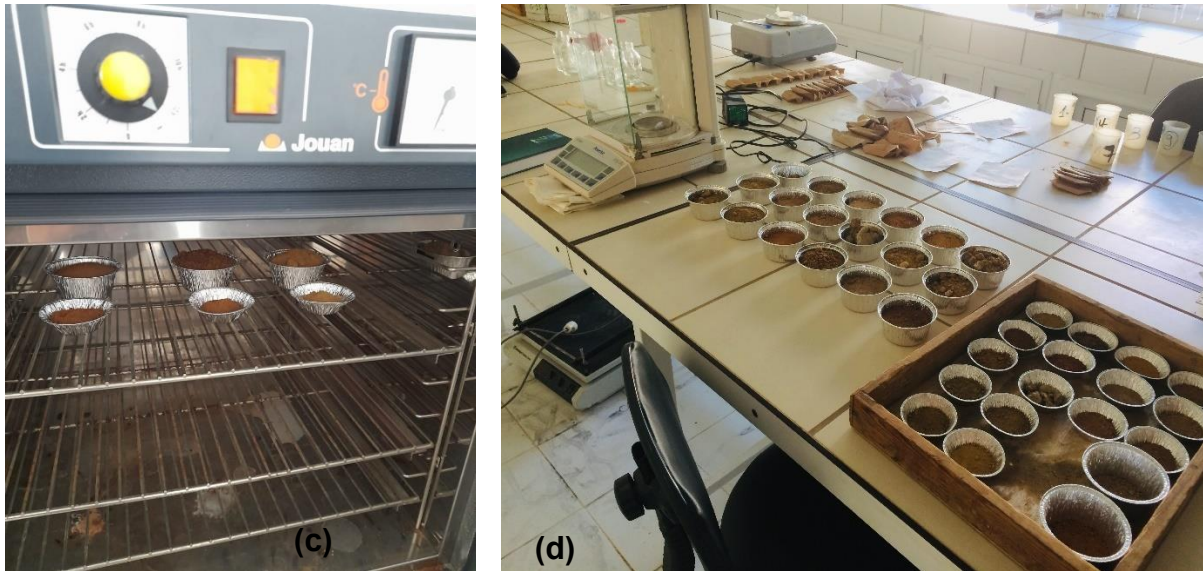


*Image 3: (a), (b), (c) and (d) illustrating steps of initial water content determination*

## 2.5. Granulometric test

The granulometric analysis of soil consists in determining the proportion of the various particle size classes. There is no perfect method to determine grain size, the accuracy of the method depends on the nature of the soil and more specifically on the geometric shape of the particles (**Rzasa and Owczarzak, 2013**). The determination of the percentage of clay and silt is based on the principle of sedimentation (**Image 4**). STOKES law expresses this speed as a function of the diameter of the particle. Clays and silts were sampled using a Robinson dropper. The determination of sand proportions was done using a dry sieving (**Pauwels et al., 1992**).



*Image 4: Sedimentation step of the granulometric test*

## **2.6. Infiltration test protocol**

### **2.6.1. Infiltration measures in the field**

The purpose of field infiltration tests is to determine the hydrodynamic parameters of the soil using measuring instruments such as infiltrometers. These tests make it possible to obtain the hydrodynamic parameters of the soil such as, hydraulic conductivity at saturation  $k_s$ , sorptivity  $S$ , or the normalization parameter of the retention curve.

During the infiltration tests, cumulative infiltration curves,  $I$ , are measured as function of time  $t$ . In general, infiltration tests are analysed using analytical functions which assume a semi-infinite medium with initial and boundary conditions.

Different instruments have been designed to perform infiltration experiments. In this work, we are interested in the simple ring infiltrometer known as Beerkan method (**Image 4**), and in the pre-defined tension disc-infiltrometer (**Image 5**).

#### **2.6.1.1. Experimental protocol for Beerkan method**

The characterization of the hydrodynamic properties of the soil by the Beerkan methodology has been widely used because it has field application with a simple ring installation (**Lassabatere *et al.*,2006**).

##### **❖ Description of the equipment**

The equipments needed for the infiltration experiments:

- Two simple rings for the infiltration
- Hammer to drive the ring into the ground
- Calibrated plastic cups for the infiltration test
- Waters cans of about 20 liters to fill the cups
- A stopwatch to measure the infiltration rates
- A spirit level to verify the horizontality of the soil



**Image 5: (a), (b), (c) and (d) illustrating steps of beerkan infiltration method**

❖ **Protocol**

The infiltration ring is sunk a few centimeters in the soil to limit water side leakage. The containers are filled with a known volume of water corresponding to a maximum water height of a few millimeters in the infiltration ring.

The experiment consists of measuring the time required for each water volume to infiltrate. At time 0, the first container is poured into the ring. A new volume is poured once the previous volume is completely infiltrated. This operation is repeated consecutively until we reach a steady state. The infiltration time of the infiltrated volume is measured with a stopwatch which only stops at the end of the test. Water can be added until two (**Mubarak *et al.*, 2009**) or three (**Mubarak *et al.*, 2010**) consecutive infiltration times are equal or until the differences in

infiltration times between consecutive water applications become negligible (**Lassabatere et al., 2019**).

The measurements correspond to the accumulation of the layers of water infiltrated as function of time. These blades are deduced by dividing the infiltrated volume by the surface of the infiltration ring.

#### ❖ **Advantages and disadvantages of the method**

The practice advantage of the protocol by **Lassabatere et al. (2006)** is the small amount of water needed for the experiment also the low cost of the materials and the simple execution.

#### **2.6.1.2. Experimental protocol for mini disk infiltrometer**

The infiltration is carried out by the methodology of a mini-disk infiltrometer (**Image 6**), with pre-set tension. The latter uses a Mariotte vessel to control the hydraulic head (**Perroux and White, 1988; Angulo-Jaramillo et al., 2000**). The tension varies between -7 and -0.5 cm.



***Image 6: Mini-disc infiltrometer apparatus***

#### ❖ **Description of the equipment**

The disk infiltrometer (**Image 6**) consists of a circular base in contact with the ground. The model we are going to use is a long infiltrometer 2.55 cm in diameter, 50 cm in length for 450 cm<sup>3</sup> of capacity, with a larger contact surface 7.75 cm in diameter for 47.17 cm<sup>2</sup> of surface.

The infiltrometer also consists of a lower chamber consisting of a water tank and a Mariotte vessel which communicates with the upper chamber. The upper chamber contains a height adjustable tube for suction control. It is limited by a stopper in its upper part and by a rubber in its lower part. The role of the Mariotte silt is to regulate the pressure in a continuous manner and not to obstruct large flows during the initial phase of the infiltration process.

#### ❖ Protocol

First, we prepare the soil surface, we prepare a flat surface on the horizon we want to perform the test (**Image 7**). During the second step, we fill both chambers with water and adjust the pressure. For the first measurement, the pressure should be low to fill the soil micropores. We note that the water level at  $t=t_0$  by a direct reading on the graduation of the water tank then we put the base of the infiltrometer in the contact with the ground and we note the time and the water level. We note the time required for the infiltration of a defined volume of water on the tank tube. We stop reading when the time difference between two successive measurements becomes constant, there we are at a steady state. The same experiment is then repeated but with a higher pressure all we need is to pull the suction tube upwards, in order to fill the macropores.



*Image 7: Field Measurements illustration*

#### ❖ Advantages and disadvantages

The pre-set tension disk infiltrometer is a lightweight and easily portable device. Measurement with this device is simple and does not require a large amount of water. It also helps to

differentiate between the volume of water that infiltrates the micropores and that which passes through the macropores. But this material is expensive and the measurement must be repeated often in space because it only concerns the surface of the soil in contact with the microporous base of the tube.

## Chapter 4: Results

### 1. Spatial distribution of the sampling points

we should mention here that our theoretical sampling points distribution, which was supposed to be done, was a map of 50 sampling points chosen. But due to many restrictions, such as COVID-pandemic, logistics, the necessary time for the experiments in each location and test that takes at least 1 hour as a minimum.

We lead till this date to 22 points done already and 12 points still working on them so that the results are not finished yet. They would be added in the final report if we can catch time.

As we can see in the map below (**Figure 13**), we worked so hard to cover the maximum possible of the upstream which of 1200 km<sup>2</sup> and to have a good recovering spatial distribution.

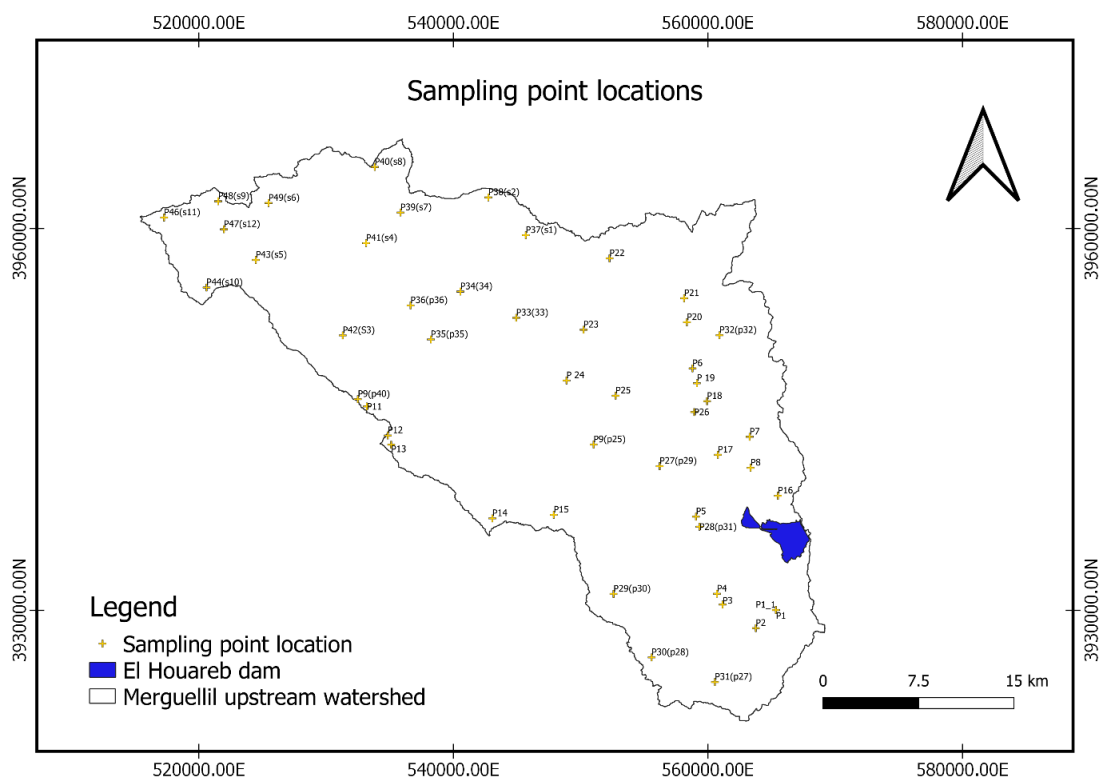


*Figure 13: Sampling points spatial distribution map*

## **2. Sampling points physicochemical characteristics**

Soil organic matter binds soil particles together into stable aggregates, carbon is the main component of soil organic matter and helps increasing porosity and infiltration. A higher content of organic matter results in better soil aggregation and improved soil structure, increasing the soil infiltration rate (Lal, 2014). Our results show that our soils contain a percentage of organic matter that varies in a range from 0.53% to 2.59%, in which the percentage of Carbone varies in a range from 0.31% to 1.50% (Table3).

Soil electrical conductivity (EC) is a measure of salts amount in soil (salinity of soil). It is an excellent indicator of nutrient availability and loss, soil texture, and available water capacity. Soils that have a higher content of small soil particles (higher content of clay) conduct more electrical current than do soils that have a higher content of larger silt and sand particles (lower content of clay). Our EC results varies in a range from 0.53 mS/cm to 2.94 mS/cm.

According to our analysis results (Table3), and the classes of salinity and EC adapted from NRCS survey Handbook (Table1, annex), our soils are non-saline to very slightly saline.

*Table 3: Physicochemical characteristics results*

Statistics	Electrical conductivity (ms/cm)	% Carbone	% Organic matter
MAX	2.94	1.50	2.59
MIN	0.53	0.31	0.53
AVERAGE	0.81	0.74	1.27

## **3. Hydraulic conductivity curves by both methods Beerkan and mini-disk infiltrometer**

### **3.1. Beerkan:**

Both the cumulative infiltration and the infiltration rate (Figure 14), showed that all measured infiltration processes were consistent with the theory of Lassabatere *et al.* (2019), because the

concavity of the cumulative infiltration as function of time curves was facing downwards and the infiltration rates decreased with time.

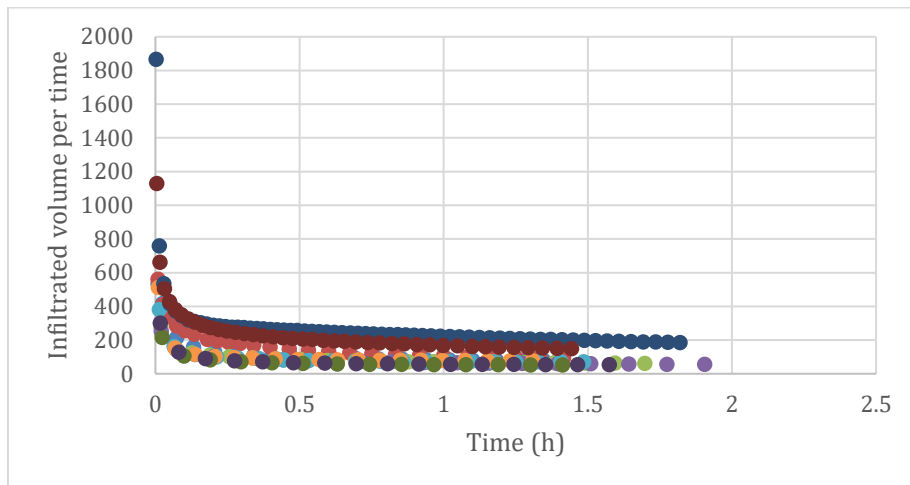


*Figure 14: Infiltration rate curves by Beerkan method*

### **3.2. Mini-disk infiltrometer:**

The gotten allure shows that all the measured infiltration process were consistent with the theory using the mini-disk infiltrometer (**Figure 15**). The difference figures in the times it takes to get to the steady-state regime and the laps between each infiltration.

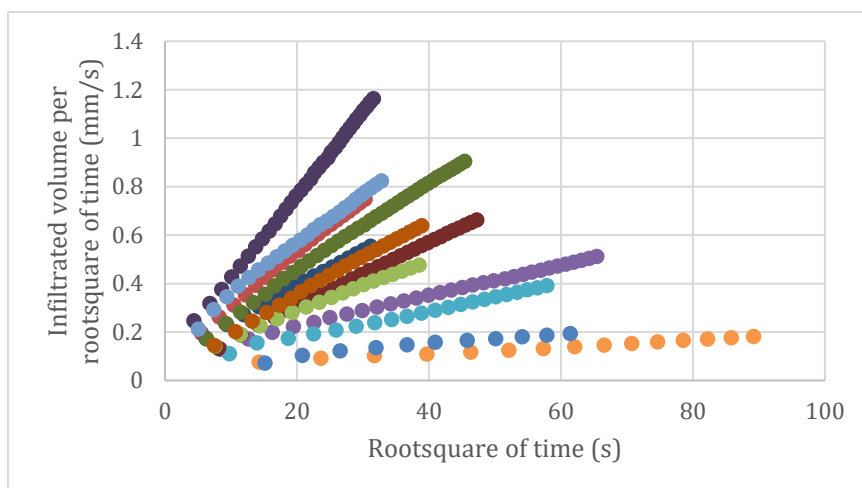


*Figure 15: Infiltration rate curves by mini-disk infiltrometer method*

#### **4. Bulk density results**

Bulk density is one of the most important parameters in studies on the soil structures. It is, in fact, linked to the nature and organization of the constituents of the soil (Chawell, 1977), and globally reflects the state of compaction of the soil. Indirectly, it makes it possible to calculate the porosity (Alongo and Kambele, 2013) which is a major characteristic controlling hydrodynamic properties of the soil (Lahlou *et al.*, 2005) and thus assess the permeability and soil water reserve (Henin *et al.*, 1969).

Natural soils can have very different bulk density ranging from 0.5 g/cm<sup>3</sup> for an organic top layer to 2.2 g/cm<sup>3</sup> for a massive mineral bottom layer. A well-structured mineral soil generally has a bulk density of about 1.3 g/cm<sup>3</sup>.

Our results show that bulk density varies from a maximum of 1.84 g/cm<sup>3</sup> to a minimum of 0.66 g/cm<sup>3</sup> (Table 4).

*Table 4: Bulk density results*

<b>Statistics</b>	<b>Bulk density</b>
MAX	1.84
MIN	0.66
AVERAGE	1.29

#### **5. Initial water content results**

Water content or moisture content is the quantity of water contained in the soil. The relationship between this parameter and the infiltration rate consists in the fact that the lower the initial soil moisture content is, the higher the initial infiltration rate is (Wei *et al.*, 2022).

The initial water content results show that we are working in almost same initial condition (dry soil). The range of values varies between a maximum of 17% and a minimum of 1% with a total average of 4% (Table 5).

*Table 5: Water initial content results*

Statistics	% Water initial content
MAX	17
MIN	1
AVERAGE	4

## **6. Granulometric results**

According to the triangle of texture mentioned before (**Figure 9**), the results show that we have in total five textural classes in our 26 analyzed samples. The soils studied are mainly loamy-sandy soils with sand percentages (**Figure 18**) that vary from 11.91% to 93.74%. The percentages of clay (**Figure 16**) vary from 1% to 39.5% and the percentages of silt vary from 2.11% to 46.38% (**Figure 17**). Soil texture is a fundamental characteristic that cannot be changed and that it has a strong relation with the infiltration rate and the hydraulic conductivity measures. Soil texture, or percentage of sand, silt and clay in the soil, is the major inherent factor affecting infiltration. Water moves more quickly through the large pores in sandy soil than it does through the small pores in clayey soil.

We used the Inverse Distance Weighted (IDW) interpolation which determines cell values using a linearly weighted combination of a set of sample points. The weight is a function of inverse distance. It assesses the predicted value by taking an average of all the known locations and allocating greater weights to adjacent points. It relies on the similarity of nearby sample points to create the surface.

To verify our results, we calculated the root mean-square of error per each pixel. The resulted value was exact of 97% to 98%. This confirms the validity of the interpolation done and the reliability of our resulted maps (**Figure 19**).

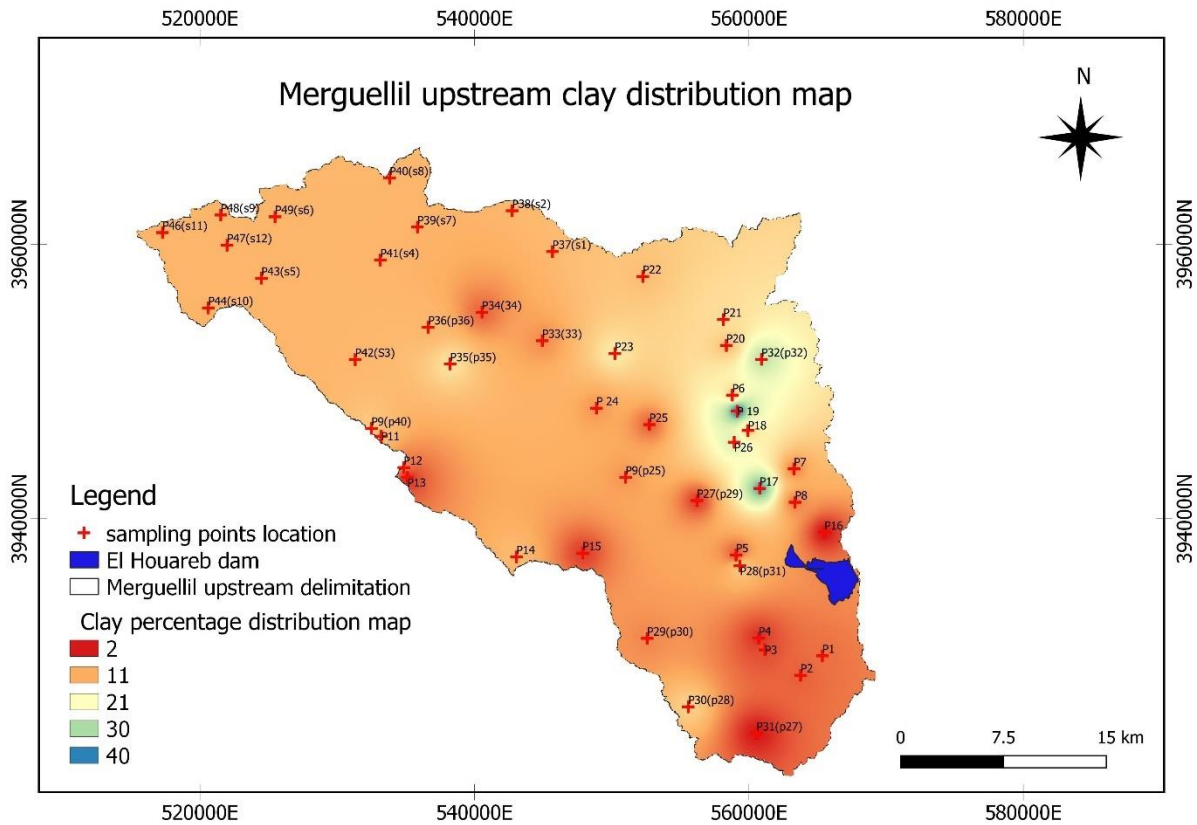


**Figure 16: Merguellil upstream clay percentage distribution map**

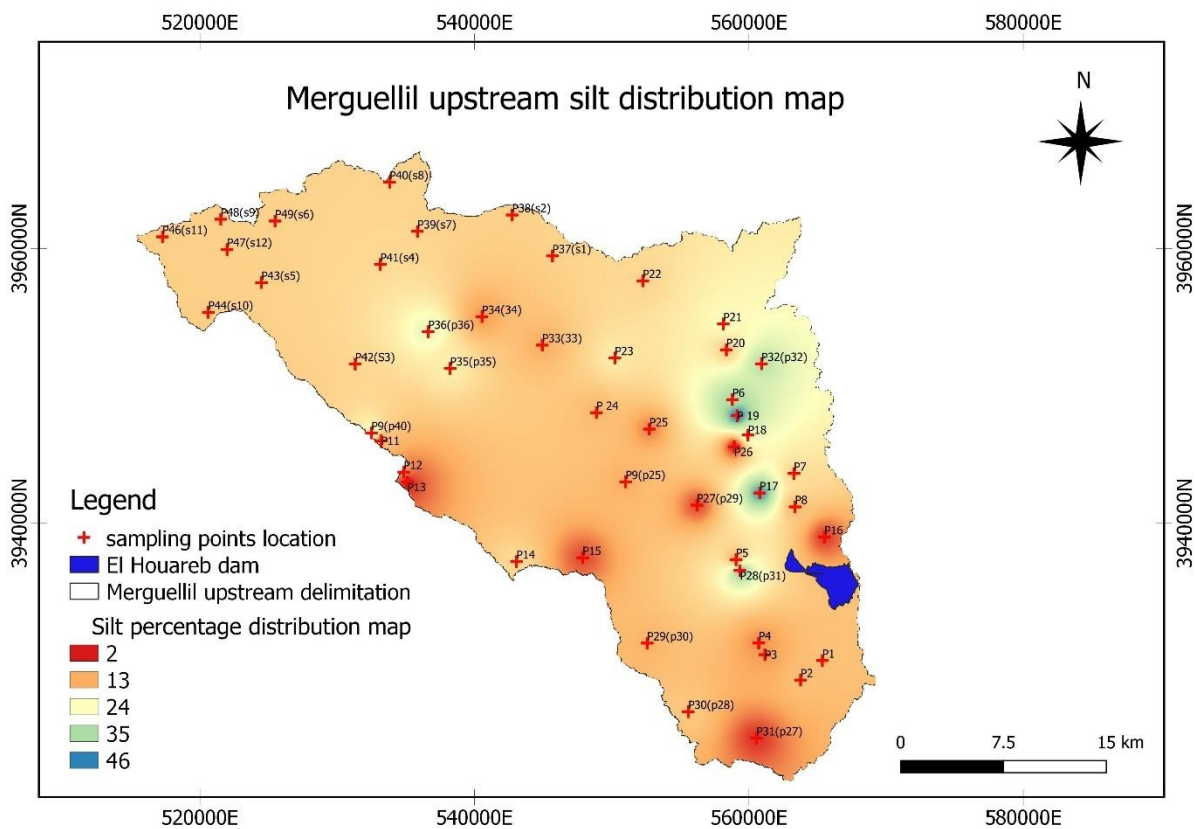


**Figure 17: Merguellil upstream silt percentage distribution map**

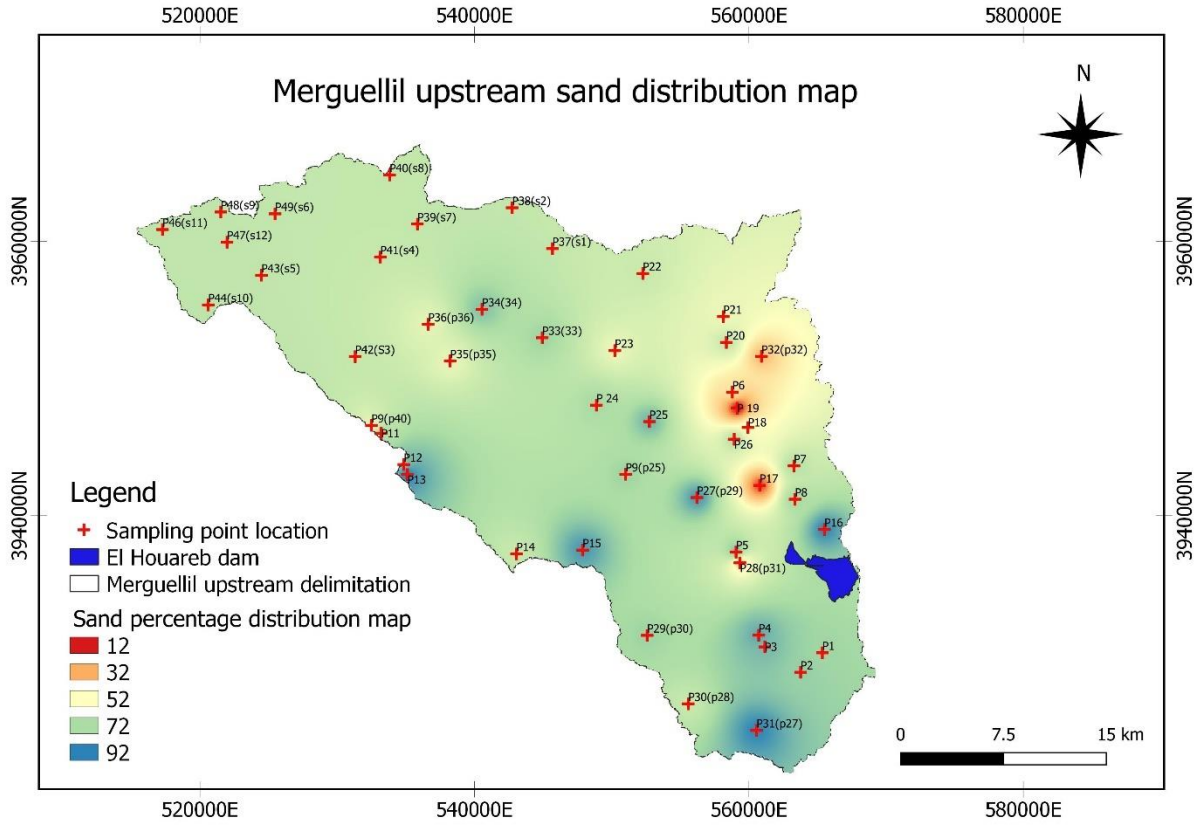


**Figure 18: Merguellil upstream sand percentage distribution map**

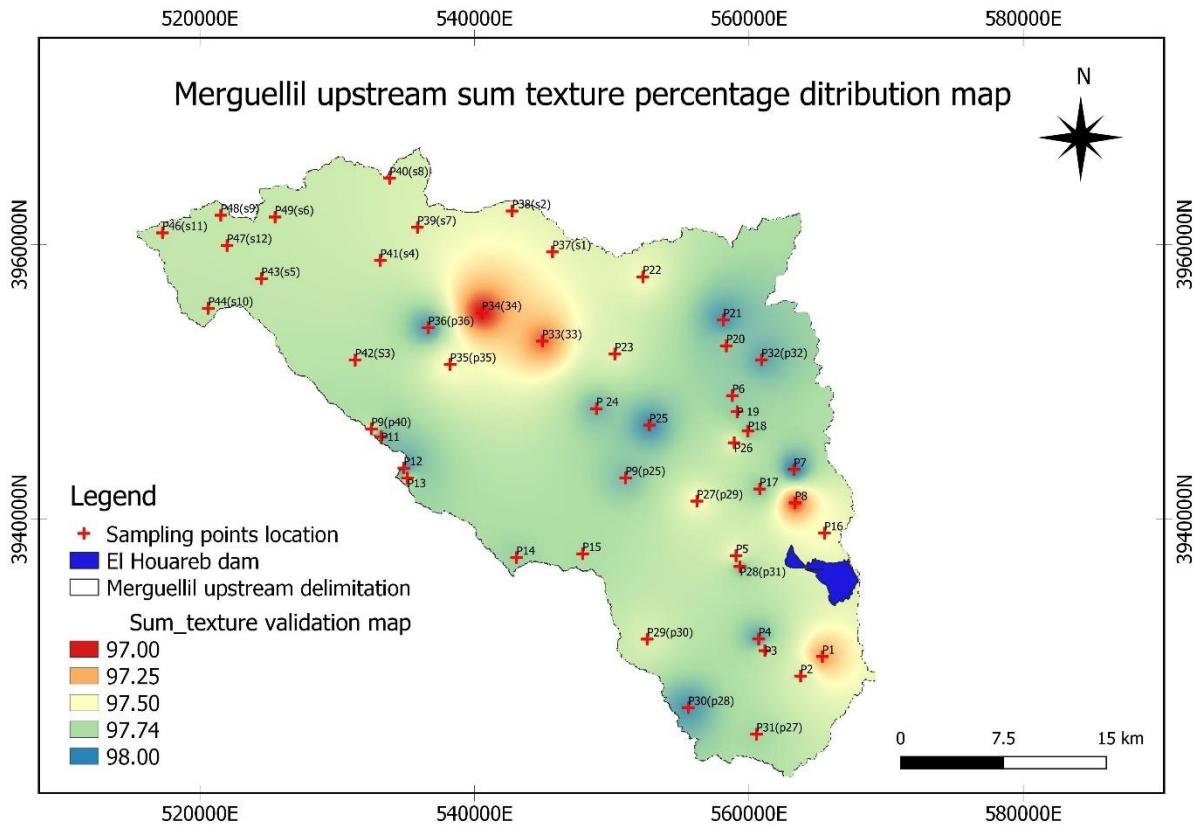


**Figure 19: Textural distribution validation map**

**Table 6: Granulometric results**

ID_points	Soil texture
P8	Loam-sand
P1	loam-sand
P2	loam-sand
P3	loam-sand
P4	loam-sand
P5	loam-sand
P6	silty
P7	loam-sand
P9-25	loam-sand
P9-40	loam-sand
P11	loam-sand
P12	loam-sand
P13	sandy
P14	loam-sand
P15	sandy
P16	sandy
P17	loamy-clay
P18	loam-sand
P19	loamy-clay
P20	loam-sand
P21	loam-sand
P22	loam-sand
P23	loam-sand
P24	loam-sand
P25	loam-sand
P26	sandy-clay-loam
P27	Sandy
P28	silty
P29(30)	sand-loam
P30(28)	loam-sand
P31(27)	sandy
P32	loam-clay
P33	loam-sand
P34	Loam-sand
P35	loam-sand
P36	loam-clay

## 7. Hydraulic conductivity map in the upstream watershed

The objective of this work is to collect data on infiltration, saturated hydraulic conductivity in the upstream part of Merguellil watershed, based on field measurements using two methods (Beerkan and mini-disc infiltrometer).

The blue-star locations (**Figure 20**) were to indicate where we have done our measurements with a back-result, due to time restrictions, we need to mention here that further results will be added as soon as possible.

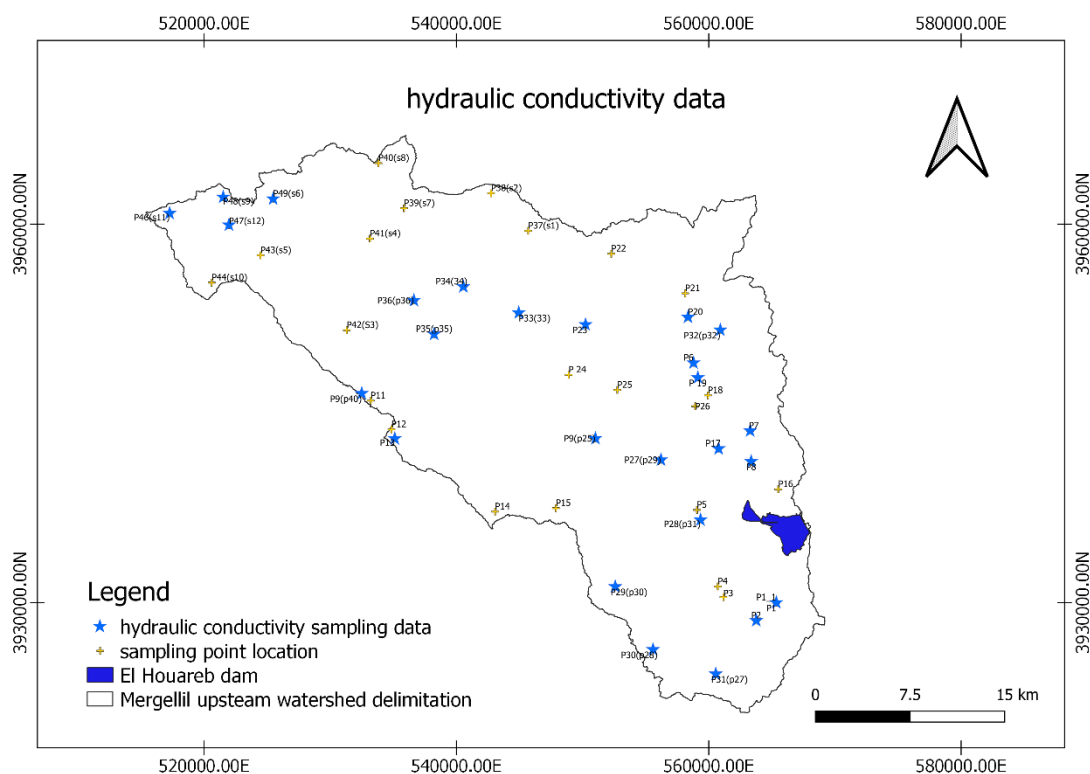


**Figure 20: Hydraulic conductivity sampling points distribution map**

Taking in consideration both; hydraulic conductivity results (Figure 21 and 22) and granulometric results (Table7), we can clearly deduce that how the infiltration rate is strongly dependent to the texture of the soil. More we are in soil where the sand percentage is higher more the hydraulic conductivity values increase and important. More the soil contains silt and clay less infiltration we have. That's indirectly related to soil structure and state. Sandy soils have bigger porous so the infiltration through it goes easier and faster than it happens in silty moreover clayey soils, which have smaller porous and less emptiness what makes the water takes longer period to go through it.

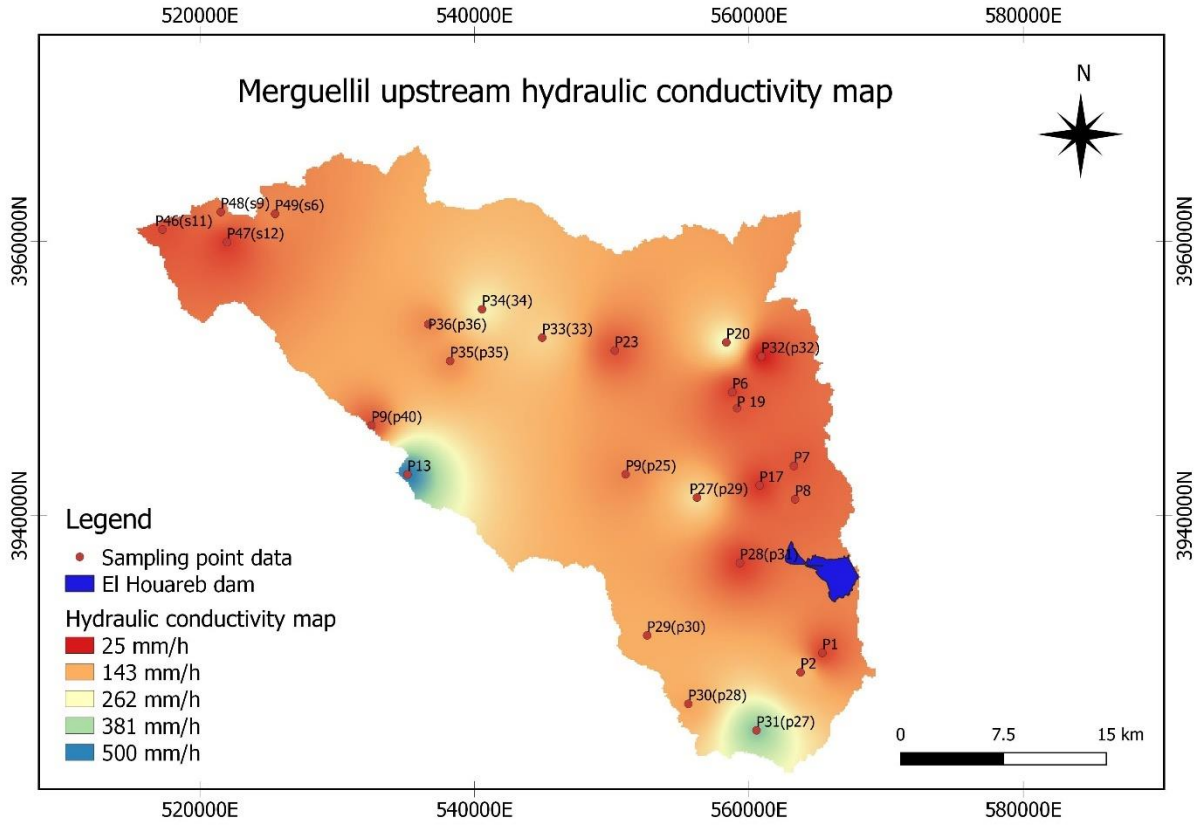


**Figure 21: Merguellil upstream hydraulic conductivity map by Beerkan method**

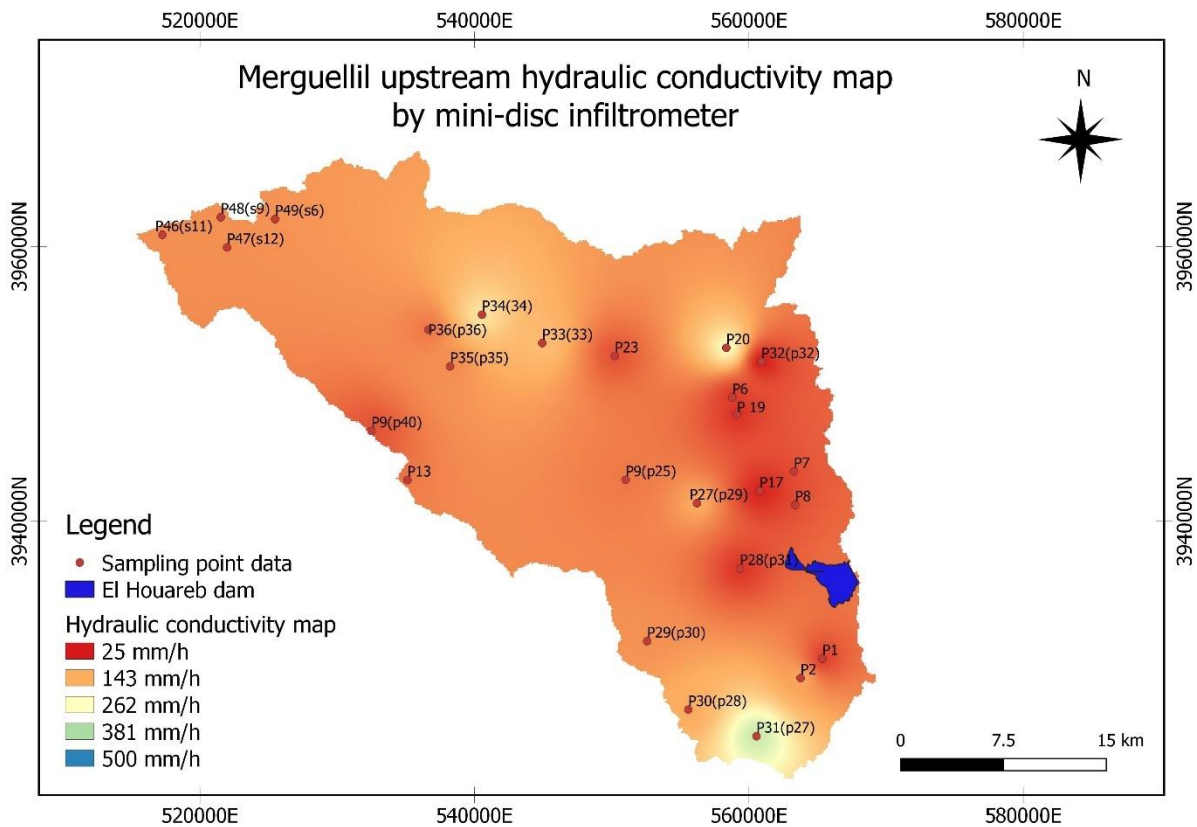


**Figure 22: Merguellil upstream hydraulic conductivity map by mini-disc infiltrometer**

## 8. Beerkan and mini-disc infiltrometer results comparison

The outcomes of both method (Beerkan and mini-disc infiltrometer) are approximately in the same range globally. Although, with the comparison of the hydraulic conductivity resulted by Beerkan and the mini-disc infiltrometer at each sampling point, we can consider that there was a little of overestimation by Beerkan method in more than one sampling point location compared to mini-disc infiltrometer method results (**Figure 23**).

The difference in hydraulic conductivity results is remarkable especially at P31 (sand soil), where Beerkan  $K_s = 405.82$  mm/h and mini-disc infiltrometer  $K_s = 334.56$  mm/h, and at P27 (sandy soil) where Beerkan  $K_s = 217.97$  mm/h and mini-disc infiltrometer  $K_s = 142.31$  mm/h. We can say that in our case, Beerkan overestimates the hydraulic conductivity compared to mini-disc infiltrometer.

At P8, P23, P30 and P35 which are loam-sand soils, we remark that Beerkan results are approximately the same as mini-disc infiltrometer results. It may be due to silt and clay presence that effect soil structuration.

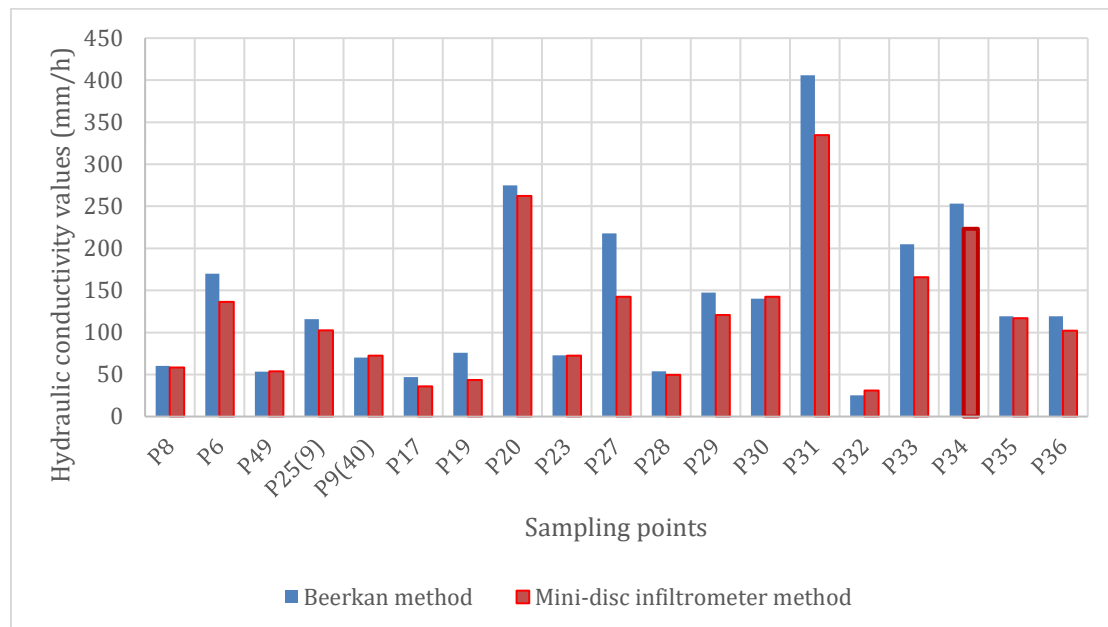


**Figure 23: Beerkan vs mini-disc infiltrometer hydraulic conductivity comparison results**

The scatter plot of hydraulic conductivity results using the two methods Beerkan and mini-disc infiltrometer (Figure24), shows a good correlation between them. The reliability of the results was assessed by the correlation coefficient (CC) that was equal to 0.96, the root mean square error (RMSE) that was equal to 23.0067 mm/h, and the Bias that was equal to 19.0014.

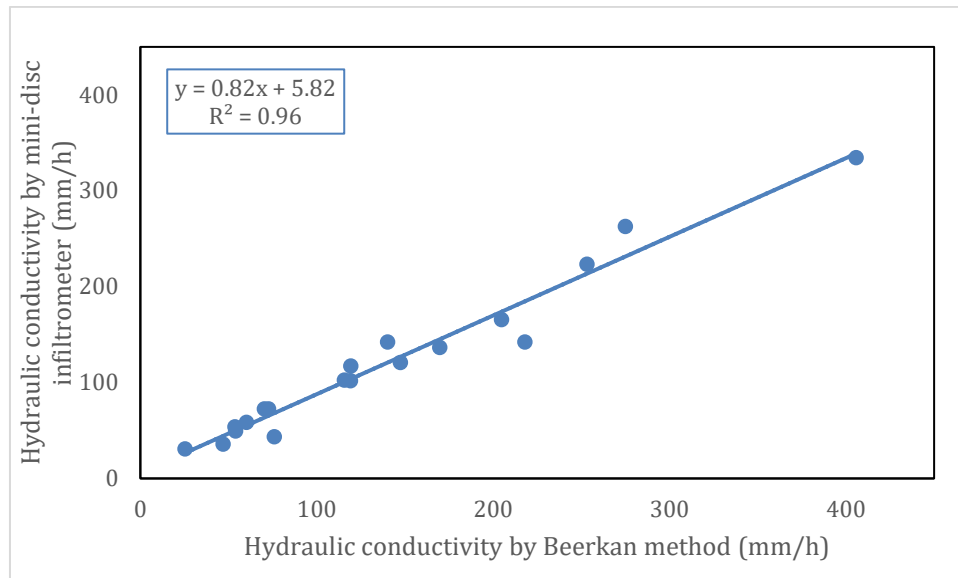


**Figure 24: Scatter plot of hydraulic conductivity results using the two methods (mini-disc infiltrometer and Beerkan)**

Stewart and Najm (2018) recently concluded that steady-state conditions using mini-disc infiltrometer may be reached in relatively short time-scales (minutes to couple of hours) even in fine textured soils. In other hand, single-ring infiltration experiments (Beerkan method), appear potentially usable to describe the soil hydrodynamic behaviour in hydrologically relevant situations and field experiments remain simple and can be completed in few hours.

## **Conclusions and perspectives**

The results elaborated in this work was the fruit of a hard work based on field data collection and field experiments. In situ experimental measurements were carried out to cover the aerial extent of the catchment despite the complex relief and the difficulties encountered to include the higher ridges.

The initial water contents, bulk density and the physicochemical parameters were evaluated through laboratory tests, for each measurement sample's location.

The hydraulic conductivity is a specific parameter of the soil. Characterizing this parameter of the unsaturated zone is mandatory for reliable modeling of flow process and effective flood/drought modeling. As a parameter, it varies strongly upon the time and space. It is very interesting to investigate its potentiality. The variability was strongly related to soil texture and structure.

The objective of this study is to evaluate infiltration characteristics based on which the saturated hydraulic conductivity values were determined. The mini-disc infiltrometer and Beerkan were the adopted methods for the filed experimental measurements.

The mini-disc infiltrometer has been more effective in some places with greater difficulty of access, and where the sand percentage is highly represented (sandy soils). In another hand, Beerkan method also has been effective in other part the only limit was the amount of water required to perform the test and the availability of water. Also, an overestimation of the hydraulic conductivity was noted in sandy soils. Otherwise, the two methods were performing good enough to be used in further studies.

We will look to develop more this research in a way that values all the data bases collected during this study work and was not totally explored.

## **References**

Adhikary SK, Muttill N, Yilmaz AG (2017) Cokriging for enhanced spatial interpolation of rainfall in two Australian catchments. *Hydrol Process* 31:2143–2161.

Alazard M. (2013). Etude des relations surface – souterrain du système aquifère d’El Haouareb (Tunisie Centrale) sous contraintes climatiques et anthropiques. Thèse de doctorat. Université Montpellier, France, 378 p.

Archer N, Bonell M, Coles N, Macdonald AM, Auton CA, Stevenson R (2013) Soil characteristics and landcover relationships on soil hydraulic conductivity at a hillslope scale: a view towards local flood management. *J Hydrol* 497:208–222.

Angulo-Jaramillo, R., J.-P. Vandervaere, S. Roulier, J.-L. Thony, J.-P. Gaudet, and M. Vauclin. (2000) Field measurement of soil surface hydraulic properties by disc and ring infiltrometers: A review and recent developments. *Soil Tillage Res.* 55:1–29.

Alongo, S. & Kambele, F., (2013). Évolution de la densité apparente et du rapport c/n du sol sous les variétés exotiques et locale de manioc dans les conditions naturelles de Kisangani (R.D.Congo). *Annales de l'Institut Facultaires des sciences agronomiques de Yangambi*, Volume 1, pp. 197-214.

Baiamonte G, Bagarello V, D’Asaro F, Palmeri V (2017) Factors influencing point measurement of near-surface saturated soil hydraulic conductivity in a small Sicilian basin. *Land Degrad Dev* 28:970–982.

Boadu FK (2000) Hydraulic conductivity of soils from grain size distribution: new models. *JGGE* 126:739–746.

Becker R, Gebremichael M, Märker M (2018) Impact of soil surface and subsurface properties on soil saturated hydraulic conductivity in the semi-arid Walnut Gulch Experimental Watershed, Arizona, USA. *Geoderma* 322:112–120.

Beskow S, Timm LC, Tavares VEQ, Caldeira TL, Aquino LS (2016) Potential of the LASH model for water resources management in data-scarce basins: A case study of the Fragata River basin, Southern Brazil. *Hydrol Sci J* 61:2567–2578.

Ben Ammar S. (2007). Contribution à l’étude hydrogéologique, géochimiques et isotopique des aquifères d’Ain El Beidha et du bassin du Merguellil (plaine de Kairouan) : implications

pour l'étude de la relation barrage – nappe. Thèse de doctorat. Université de Sfax, Tunisie, 202 p.

**Ben Boubaker H, Benzarti Z, Hénia L. (2003).** Les ressources en eau de la Tunisie : contraintes du climat et pression anthropique. Eau et environnement. Tunisie et milieux méditerranéens. ENS Lyon éditions, Collection Sociétés, Espaces temps, France, 208 p.

**Bouzaiane S, Lafforgue A. (1986).** Monographie hydrologique des oueds Zeroud et Merguellil. DGRE, ORSTOM : Tunis, Tunisie, 1058 p.

**Ben Mansour H. (2006).** Evolution des aménagements de conservation des eaux et des sols dans le bassin amont du Merguellil, Tunisie centrale. Direction générale des ressources en eau, Tunisie, 83 p.

**Bockhorn, B.; Klint, K.E.S.; Locatelli, L.; Park, Y.-J.; Binning, P.J.; Sudicky, E.; Bergen Jensen, M. (2017)** Factors affecting the hydraulic performance of infiltration-based SUDS in clay. *Urban Water J.*, 14, 125–133.

**Blake, G.R., et K.H. Hartge. (1986)** Bulk Density. *Methods of Soil Analysis, Part 1, Soil Sci. Soc. Am.*, pp. 363-376, Madison, WI, USA.

**Barbery, J.; Mohdi, M. (1987)** Carte des Ressources en Sols de la Tunisie, Feuille de Kairouan; Direction des ressources en eau et en sol: Division des sols, Tunisie; p 53.

**Cressie N, Hawkins DM (1980)** Robust estimation of the variogram: I. *Math Geol* 12:115–125.

**Calvet, R., (2003).** Le sol : Propriétés et fonctions, Tome 2 : Phénomènes physiques et chimiques, Applications agronomiques et environnementales. Dunod et éditions France Agricole, 511p.

**Chadly B. (1992)** Note sur l'évolution de la nappe de Kairouan après la fermeture du barrage d'El Haouareb. 24 pages.

**De Gruijter, J.J. (2002)** Sampling. In J.H. Dane and G.C. Topp, Eds. *Methods of Soil Analysis, Part 4—Physical Methods*. Soil Science Society of America, Inc., Madison, WI, pp. 45–79.

**Das Gupta, S.; Mohanty, B.P.; Köhne, J.M. (2006)** Soil Hydraulic Conductivities and their Spatial and Temporal Variations in a Vertisol. *Soil Sci. Soc. Am. J.*, 70, 1872–1881.

**Deb, S.K.; Shukla, M.K. (2012)** Variability of hydraulic conductivity due to multiple factors. *Am. J. Environ. Sci.*, 8, 489–502.

- Dridi B.** (2000). Impact des aménagements sur la disponibilité des eaux de surface dans le bassin versant du Merguellil (Tunisie centrale). Thèse de doctorat. UFR de Géographie, Centre d'études et de recherche eco-géographiques - CEREG UMR 7007, CNRS/ULP/ENGESS. Université Louis Pasteur. 194 p.
- Duval E.** (1971). Essai pour reconstituer un historique des crues du Merguellil de l'an 861 à 1971. Rapport Tech. Division des Ressources en Eau. Tunis. 85 p.
- FIDA** (2004). Projet de développement agricole et rural intégré de Siliana (PDARI). Agence Française de Développement. Evaluation report. Rapport n° 1569. 100 p.
- Guellouz, L. ; Askri, B. ; Jaffré, J. ; Bouhlila, R.** (2020). Estimation of the soil hydraulic properties from field data by solving an inverse problem. *Sci. Rep.*, 10, 9359.
- Goovaerts P** (1997) Geostatistics for natural resources evaluation. Applied Geostatistics Series. Oxford University Press, Oxford.
- Gilbert, R.O.** (1987) Statistical Methods for Environmental Pollution Monitoring. Van Nostrand Reinhold, New York, NY, 320 pp.
- Grela, R., D. Xanthoulis, J.M. Marcoen, M. Lemineur, M. Wauthélet.** (2004) L'infiltration des eaux usées épurées. Guide pratique. Convention d'étude entre la FUSAG, l'INASEP et la DGRNE « Etude de méthodes et d'outils d'aide à la décision pour la planification et la mise en œuvre de systèmes d'épuration individuelle ou groupée », 29 p.
- Henin S., Monnier G., Gras R.,** (1969) - Le profil cultural. Masson, Paris, 2<sup>e</sup> édition, 332 pp.
- Hamza M.** (1983) Les ressources en eau du Kairouannais, identification et évaluation, mobilisation et allocation. 20 pages.
- Hamza M.** (1988). Projet de développement agricole du gouvernorat de Kairouan (Ressources en eau). Rapp. Tech. D.G.R.E., Tunis, 90 p.
- Hamza M.** (1976). Contribution à l'étude hydrogéologique du synclinal d'Aïn El Beidha. Thèse de Doctorat. Université de Paris VI, Paris, France, 281p.
- Hillel, D.** (1998) Environmental Soil Physics: Fundamentals, Applications, and Environmental Considerations. Academic Press, Waltham.

**Hu W, Dongli S, Ming'an S, Kwok PC, Bingcheng S (2015)** Effects of initial soil water content and saturated hydraulic conductivity variability on small watershed runoff simulation using LISEM. *Hydrol Sci J* 60:1137–1154.

**INM. (2019).** Institut National de la Météorologie.

**Jenny H (1941)** Factors of soil formation: a system of quantitative pedology. Dover Publications, New York.

**Jacques, D., B.P. Mohanty and J. Feyen. (2002)** Comparison of alternative methods for deriving hydraulic properties and scaling factors from single-disc tension infiltrometer measurements. *Water Resour. Res.* 38:25.1–25.14.

**Kanso, T.; Tedoldi, D.; Gromaire, M.-C.; Ramier, D.; Saad, M.; Chebbo, G. (2018)** Horizontal and Vertical Variability of Soil Hydraulic Properties in Roadside Sustainable Drainage Systems (SuDS)—Nature and Implications for Hydrological Performance Evaluation. *Water*, 10, 987.

**Kingumbi A. (2006).** Modélisation hydrologique d'un bassin affecté par des changements d'occupation. Cas du Merguellil en Tunisie centrale. Thèse de Doctorat, Ecole nationale d'ingénieurs de Tunis, Tunis, Tunisie, 218 p.

**Lal Rattan. (2014).** Soil Carbon Management and Climate Change. *Carbon Management.* 4. 439-462. 10.4155/cmt.13.31.

**Lin H (2006)** Temporal stability of soil moisture spatial pattern and subsurface preferential flow pathways in the Shale Hills catchment. *Vadose Zone J* 5:317–340.

**Libohova Z, Schoeneberger P, Bowling LC, Owens PR, Wysocki D, Wills S, Williams CO, Seybold C (2018)** Soil systems for upscaling saturated hydraulic conductivity for hydrological modeling in the critical zone. *Vadose Zone J* 17:170051.

**Lark RM (2000)** A comparison of some robust estimators of the variogram for use in soil survey. *Eur J Soil Sci* 51:137–157.

**Lebrenz H, Bárdossy A (2017)** Estimation of the variogram using Kendall's tau for a robust geostatistical interpolation. *J Hydrol Eng* 22:38–46.

**Lark RM (2003)** Two robust estimators of the cross-variogram for multivariate geostatistical analysis of soil properties. *Eur J Soil Sci* 54: 187–202.

- Leduc C, Ben Ammar S, Favreau G, Béji R, Virrion R, Lacombe G, Tarhouni J, Aouadi C, Zenati Chelli B, Jebnoun N, Oi M, Michelot JL, Zouari K. (2007). Impacts of hydrological changes in the Mediterranean zone: environmental modifications and rural development in the Merguellil catchment, central Tunisia. *Hydrological Sciences Journal* 52(6): 1162–1178.
- Lacombe G, Cappelaere B, Leduc C. (2008). Hydrological impact of water and soil conservation works in the Merguellil catchment of central Tunisia. *Journal of Hydrology* 359 : 210-224.
- Lassabatère, L.; Di Prima, S.; Angulo-Jaramillo, R.; Keesstra, S.; Salesa, D. (2019) Beerkan multi-runs for characterizing water infiltration and spatial variability of soil hydraulic properties across scales. *Hydrolog. Sci. J.* 64: 165-78.
- Lassabatère, L.; Angulo-Jaramillo, R.; Ugalde, J.M.S.; Cuenca, R.; Braud, I.; Haverkamp, R. (2006) Beerkan estimation of soil transfer parameters through infiltration experiments: BEST. *Soil Sci. Soc. Am. J.*, 70, 521–532.
- Lahlou, S. et al., (2005) Modification de la porosité du sol sous les techniques culturales de conservation en zone semi-aride Marocaine. *Etude et Gestion des Sols*, XII, 1, pp. 69-76.
- Mubarak, I., Mailhol J.C., Angulo-Jaramillo R., Ruelle P., Boivin P., Khaledian M. (2009) *Geoderma*, 150: 158-65.
- Mubarak, I.; Angulo-Jaramillo, R.; Mailhol, J.C.; Ruelle, P.; Khaledian, M.; Vauclin, M. (2010) Spatial analysis of soil surface hydraulic properties: Is infiltration method dependent? *Agric. Water Manag.*, 97, 1517–1526.
- Mechy J. (2013). Cartographie des travaux de CES (banquettes et lacs collinaires) dans le bassin versant. *Projet de fin d'étude*. Institut National Agronomique de Tunisie, Tunisie, 84p.
- Maier, F., van Meerveld, I., Greinwald, K., Gebauer, T., Lustenberger, F., Hartmann, A., Musso, A., (2020). Effects of soil and vegetation development on surface hydrological properties of moraines in the Swiss Alps. *CATENA* 187, 104353.
- Mizouri M., Barbery J. et Willaine P. (1990) Carte des ressources en sols de la Tunisie (1/200000) : nouvelle approche méthodologique, feuille de Makthar. Tunis, Ministère de l'agriculture.

Nasri S, (2007). Cracteristiques et impacts hydrologiques de banquettes en cascade sur un versant semi-aride en Tunisie centrale. *Hydrological Sciences Journal* 52 (6), 1134–1145 p.

Ogilvie A, Le Goulven P, Leduc C, Calvez R, Mulliga M. (2014). Réponse hydrologique d'un bassin semi-aride aux événements pluviométriques et aménagements de versant (bassin du Merguellil, Tunisie centrale) *Hydrological Sciences Journal* 61 (1) : 441-453.

Ouali J. (1985) Structure et évolution géodynamique du chañon Nara-sidi Khalif (Tunisie centrale). *Bulletin - Centre de Recherches Exploration - Production Elf - Aquitaine* 9, 1 : 155-182.

Parr, J. F. & Bertrand, A. R. (1960) Water infiltration in soils [Abstract]. *Advances in Agronomy*, 12, 311-363.

Perroux K.M. and White I., (1988) Designs for disk permeameters. *Soil Sci. Soc. Am. J.*, 52:1205-1215.

Philip (I.R.), (1957) The theory of infiltration: 4. Sortivity and algebric infiltration equations. *Soil Scie.*; 84: 257-264.

Papanicolaou AN, Elhakeem M, Wilson CG, Burras CL, West LT, Lin H, Clark B, Oneal BE (2015) Spatial variability of saturated hydraulic conductivity at the hillslope scale: Understanding the role of land management and erosional effect. *Geoderma* 243–244:58–68.

Picciafuoco T, Morbidelli R, Flammini A, Saltalippi C, Corradini C, Strauss P, Blöschl G (2019) A pedotransfer function for field-scale saturated hydraulic conductivity of a small watershed. *Vadose Zone J* 12:1–15.

Pinto LC, Mello CR, Norton LD, Curi N (2019) Land-use influence on the soil hydrology: an approach in upper Grande River basin, Southeast Brazil. *Ciênc Agrotec* 43: e015619.

Price K, Jackson CR, Parker AJ (2010) Variation of surficial soil hydraulic properties across land uses in the southern Blue Ridge Mountains, North Carolina, USA. *J Hydrol* 383:256–268.

Qiao JB, Zhu YJ, Jia X, Huang LM, Shao MA (2018) Estimating the spatial relationships between soil hydraulic properties and soil physical properties in the critical zone (0–100 m) on the Loess Plateau, China: a state-space modeling approach. *Catena* 160:385–393.

Reichardt K, Timm LC (2020) *Soil, plant and atmosphere: concepts, processes and applications*. Springer, Basel.

Simonson RW (1959) Outline of a generalized theory of soil genesis<sup>1</sup>. *Soil Sci Soc Am J* 23:152–156.

She D, Qian C, Timm LC, Beskow S, Wei H, Caldeira TL, Oliveira LM (2017) Multi-scale correlations between soil hydraulic properties and associated factors along a Brazilian watershed transect. *Geoderma* 286:15–24.

Salemi LF, Groppo JD, Trevisan R, Moraes JM, Ferraz SFB, Villani JP, Duarte-Neto PJ, Martinelli LA (2013) Land-use change in the Atlantic rainforest region: consequences for the hydrology of small catchments. *J Hydrol* 499:100–109.

Song X, Chen X, Ye M, Dai X, Hammond G, Zachara JM (2019) Delineating facies spatial distribution by integrating ensemble data assimilation and indicator Geostatistics with level-set transformation. *Water Resour Res* 55:2652–2671.

Santra, P., Chopra, U., Chakraborty, D., (2008). Spatial variability of soil properties and its application in predicting surface map of hydraulic parameters in an agricultural farm. *Curr. Sci.* 95 ;7, 937–945.

Sobieraj, J.A., Elsen beer, H., Coelho, R. M., Newton, B., (2002) Spatial variability of soil hydraulic conductivity along a tropical rain forest catena. *Geoderma* 108, 79–90.

Stewart. R.D., Najm. M.R.A., (2018) A Comprehensive Model for Single Ring Infiltration I: Initial Water Content and Soil Hydraulic Properties. *Soil Sci. Soc. Am. J*, 82: 548-57.

Wooding R.A., (1968) Steady infiltration from a shallow circular pond. *Water Resour. Res.* 4:1259-1273.

Wallin J, Bolin D (2015) Geostatistical modelling using non-gaussian matérn fields. *Scand J Stat* 42:872–890.

Wang Y, Shao M, Liu Z, Horton R (2013) Regional-scale variation and distribution patterns of soil saturated hydraulic conductivities in surface and subsurface layers in the loessial soils of China. *J Hydrol* 487:13–23.

Wang Z, Shi W (2018) Robust variogram estimation combined with isometric log-ratio transformation for improved accuracy of soil particle-size fraction mapping. *Geoderma* 324:56–66.

Wei, L.; Yang, M.; Li, Z.; Shao, J.; Li, L.; Chen, P.; Li, S.; Zhao, R. (2022). Experimental Investigation of Relationship between Infiltration Rate and Soil Moisture under Rainfall Conditions. *Water*, 14, 1347.

Yang Y., and Wendroth O. (2014). State-space approach to analyze field-scale bromide leaching. *Geoderma*. 217-218:161–172.

Zimmermann, A., Schinn, D.S., Francke, T., Elsenbeer, H., and Zimmermann, B., (2013). Uncovering patterns of near-surface saturated hydraulic conductivity in an overland flow-controlled landscape. *Geoderma*, 195–196, 1–11. doi: 10.1016/j.geoderma.2012.11.002.

Zhang, Y., Schaap, M.G., (2019). Estimation of saturated hydraulic conductivity with pedotransfer functions: A review. *J. Hydrol.* 575, 1011–1030.

Suggested citation: Hmaied Asma. (2023). The spatial distribution of the saturated hydraulic conductivity in the upstream part of the Merguellil watershed for the improvement of the hydrological modeling. [Zenodo]. <https://doi.org/10.5281/zenodo.8046867>

## Annex:

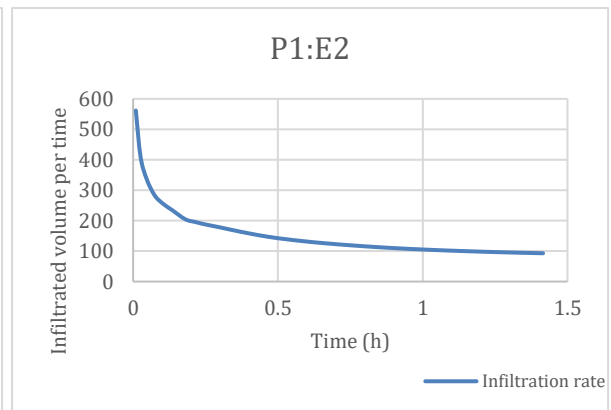
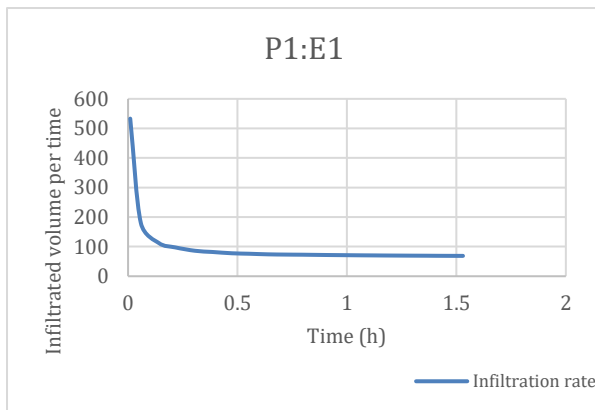
*Table 1. Classes of salinity and EC (1 dS/m = 1 mmhos/cm; adapted from NRCS Soil Survey Handbook)*

EC (dS/m)	Salinity Class
0 < 2	Non-saline
2 < 4	Very slightly saline
4 < 8	Slightly saline
8 < 16	Moderately saline
≥ 16	Strongly saline

Examples

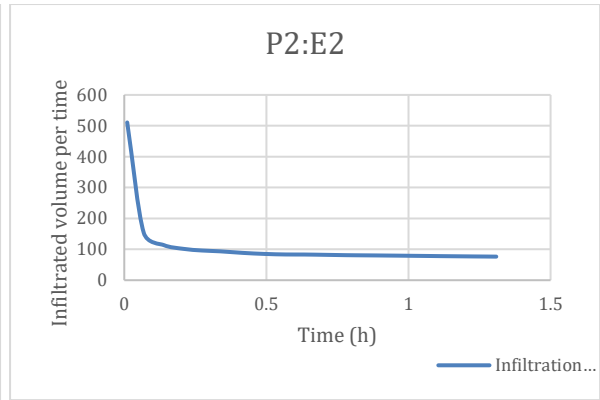
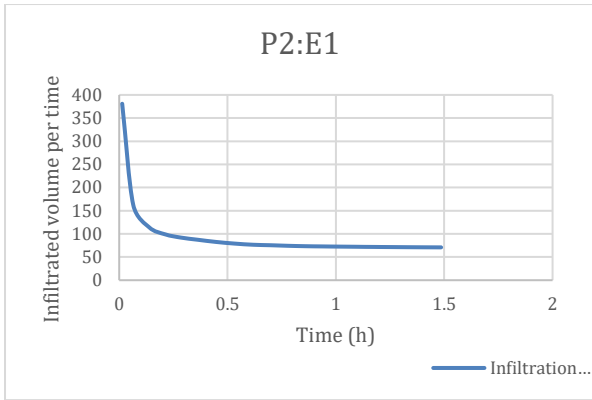
### Location 1

Beerkan results



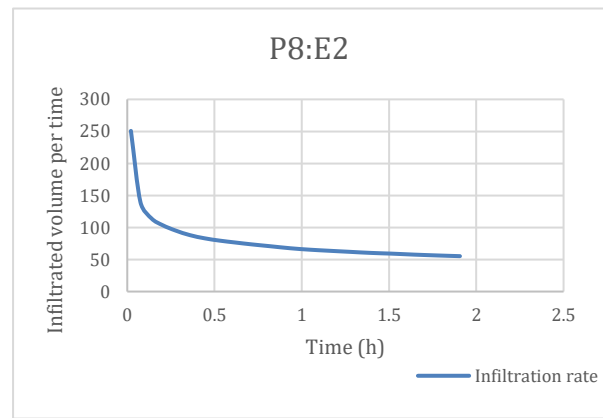
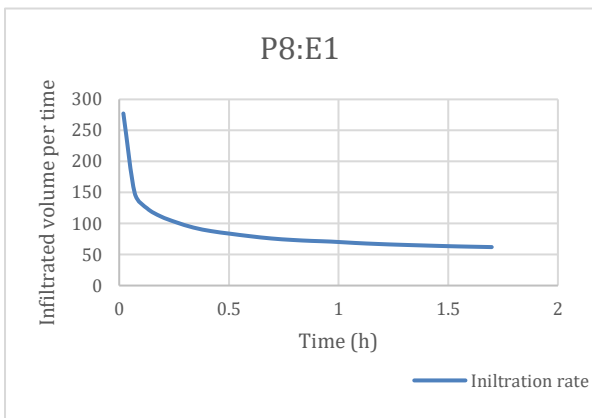
### Location 2

Beerkan results



**Location 3**

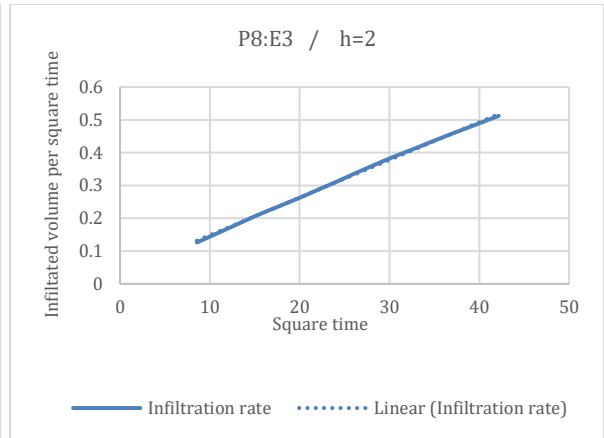
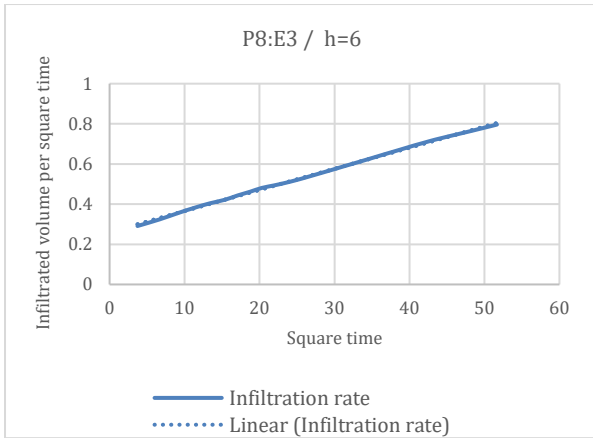
Beerkan results



Mini disk infiltrometer results

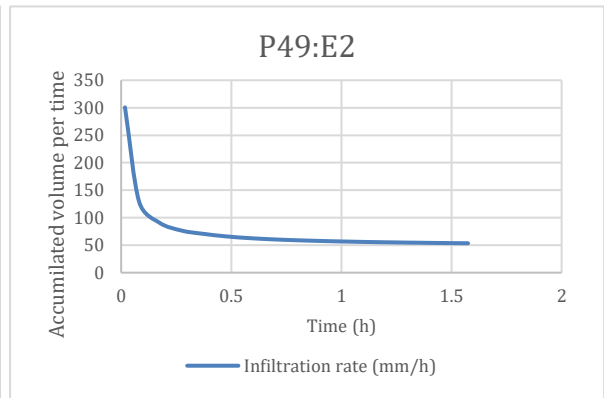
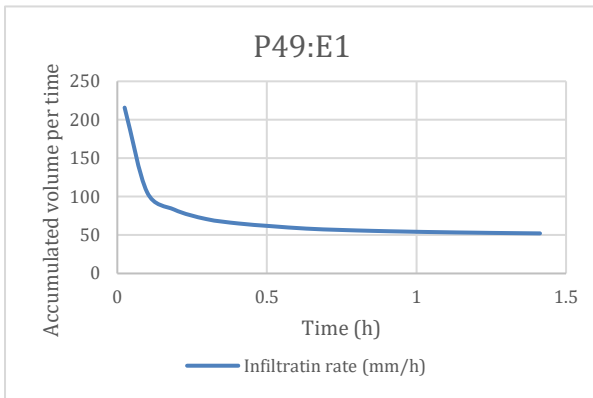
At tension 6

At tension 2



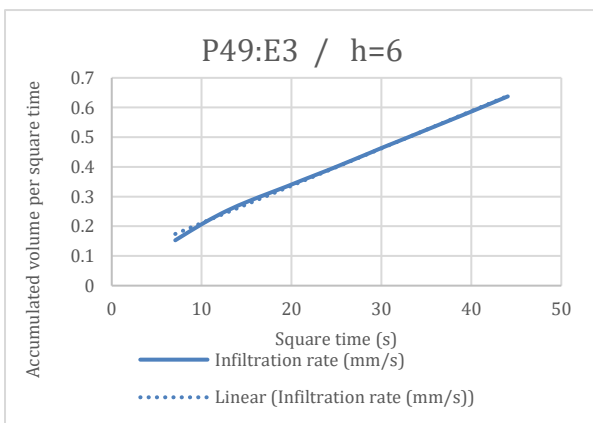
**Location 5**

Beerkan results

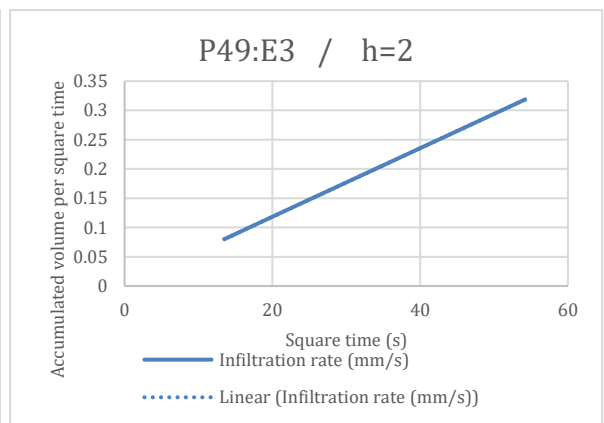


Mini disk infiltrometer results

At tension 6

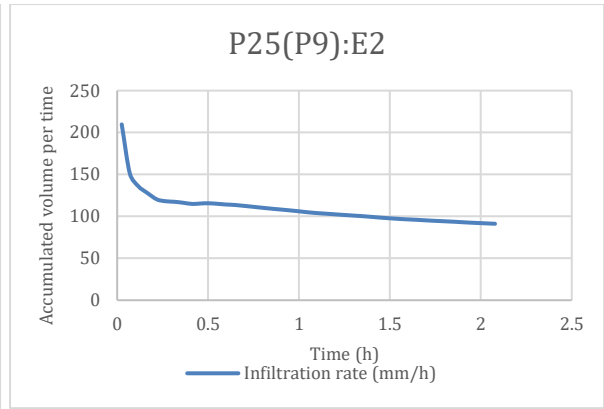
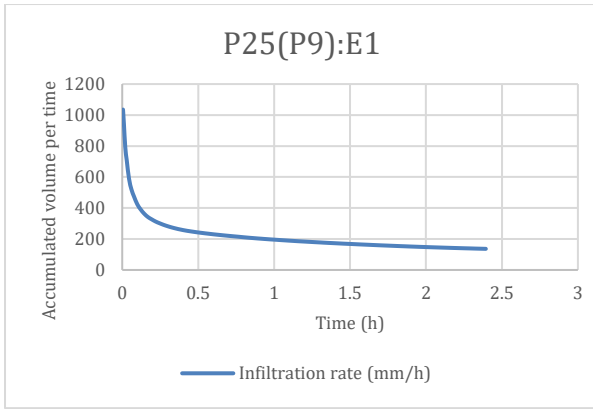


At tension 2



**Location 6**

Beerkan results



Mini disk infiltrometer results

At tension 6

At tension 2

